

Gauge-Aligned Graviton Emergence (GAGE): Deriving a Running G from Standard Model Couplings

[Michael DeMasi, DNP]¹

¹/Independent

(Dated: October 28, 2025)

Within the Standard Model at $\mu = M_Z$ ($\overline{\text{MS}}$), a unique primitive projector $\chi = (16, 13, 2)$ defines the gauge-log depth $\Xi = \chi \cdot \hat{\Psi}$. Enforcing an even curvature gate $\Pi(\Xi) = \exp[-(\Delta\Xi)^2/\sigma_\chi^2]$ with $\Pi'(\Xi_{\text{eq}}) = 0$ produces a GR-normalized, massless tensor sector ($m_{\text{PF}} = 0$) and a running coupling $G(x) = G\Pi(\Xi(x))$ where

$$G = \frac{\Omega \hbar c}{m_p^2}, \quad \Omega = \hat{\alpha}_s^{16} \hat{\alpha}_2^{13} \hat{\alpha}^2$$

(hats denote $\overline{\text{MS}}$ values at $\mu = M_Z$). Two falsifiers follow: a quadratic lab-null $\Delta G/G \simeq (\Delta\Xi/\sigma_\chi)^2$ and the closure/leave-one-out tests ($\Omega/\alpha_G^{(\text{pp})} = 1.09373393$, $\hat{\alpha}_s^*(M_Z) = 0.1173411 \pm 1.86 \times 10^{-5}$). All inputs are SM-pinned; metrology enters only *a posteriori*.

Motivation. Despite its precision, the Standard Model has not yielded a self-contained derivation of Newton's constant G_N or a massless spin-2 graviton within its gauge structure. We propose an *alignment principle*: near the electroweak scale, the gauge system aligns along the soft eigenmode of the equilibrium kinetic metric, rendering the curvature response parity-even at the laboratory point. At $\mu = M_Z$ in $\overline{\text{MS}}$, an SNF-certified projector $\chi = (16, 13, 2)$ fixes the gauge-log depth $\Xi = \chi \cdot \hat{\Psi}$; enforcing an even gate $\Pi(\Xi)$ with $\Pi'(\Xi_{\text{eq}}) = 0$ yields a GR-normalized, massless spin-2 sector with no new fields or tunable parameters and defines an emergent gravitational coupling G . The framework is parameter-free and falsifiable: defining $s_\Xi \equiv \Delta\Xi/\sigma_\chi$, $\phi_\chi \equiv \Delta\Xi/\|\chi\|_{\mathbf{K}_{\text{eq}}}$, $\Lambda_{\text{gate}} \equiv \sigma_\chi/\|\chi\|_{\mathbf{K}_{\text{eq}}}$ gives $\Delta G/G = s_\Xi^2 = (\phi_\chi/\Lambda_{\text{gate}})^2$; closure is tested *a posteriori* against metrology through $\alpha_G^{(\text{pp})} = G_N m_p^2/(\hbar c)$.

Premise. Work in the logarithmic coupling space $\hat{\Psi} = (\ln \hat{\alpha}_s, \ln \hat{\alpha}_2, \ln \hat{\alpha})$, where multiplicative renormalization becomes additive and basis transports are linear [1–3]. We seek a *single*, basis-invariant scalar depth in this space that governs the curvature response and defines the emergent coupling $G(x)$. Its existence is not postulated but must arise from Standard-Model structure and be protected by a symmetry ensuring an even equilibrium response (*i.e.*, a null first derivative).

Alignment principle (physical motivation). Let $\mathbf{K}_{\text{eq}} \succ 0$ denote the equilibrium kinetic metric on $\hat{\Psi}$. Small variations organize along the *soft eigenmode* of \mathbf{K}_{eq} —the direction of minimal kinetic curvature. We propose, and verify numerically using SM pins [4, 5], that the gauge system aligns its response along this soft mode. Alignment has two direct consequences: (i) **Parity protection.** Near equilibrium, the response is even, so the leading deviation is quadratic in the depth displacement. The resulting *parity-null* is directly testable—any observed linear term would falsify the mechanism (symbols such as $\Delta\Xi$ and σ_χ are defined below). (ii) **Tensor-sector normalization.** With even parity at the laboratory point,

the linearized tensor dynamics coincide with GR (luminal helicity-2, no Pauli–Fierz mass). Thus, the graviton sector is not added by hand but emerges as the parity-even curvature response of the aligned gauge system [6, 7]. This alignment-first view provides the physical intuition before the algebra. The next sections formalize it by identifying the unique direction (certificate), defining the depth Ξ , specifying an even curvature gate $\Pi(\Xi)$, deriving the β -function for G , and establishing closure and falsifiers.

In Fisher-metric terms, alignment corresponds to motion along the soft eigenvector of \mathbf{K}_{eq} —the direction of least informational curvature. Equivalently, systems minimize Fisher resistance by cohering along the soft mode, the information-geometry analog of least action.

Integer certificate and depth. The alignment principle requires a single scalar coordinate in coupling space that remains invariant under renormalization–basis changes. From the one-loop decoupling lattice of the Standard Model, the Smith normal form (SNF) isolates a unique primitive left-kernel generator [8–10]

$$\chi = (16, 13, 2), \quad (1)$$

certifying that only one integer combination of gauge couplings remains invariant under one-loop decoupling transformations (Appelquist–Carazzone regime) [8]. This integer projector defines the gauge-log depth

$$\Xi = \chi \cdot \hat{\Psi}, \quad \hat{\Psi} = (\ln \hat{\alpha}_s, \ln \hat{\alpha}_2, \ln \hat{\alpha}), \quad (2)$$

with local fluctuation $\Delta\hat{\Xi} = \Xi - \hat{\Xi}^{(\text{eq})}$. Log coordinates render multiplicative renormalization additive and basis transports linear [1, 2]: $\hat{\Psi}' = A\hat{\Psi}$, $\chi' = A^{-\top}\chi$, so $\Xi = \chi \cdot \hat{\Psi}$ is basis-invariant. Under metric transport $K' = A^{-\top}KA^{-1}$ one finds

$$\|\chi\|_K^2 = \chi^\top K \chi = \chi'^\top K' \chi', \quad (3)$$

so the norm $\|\chi\|_K$ and hence the gate scale $\Lambda_{\text{gate}} = \sigma_\chi/\|\chi\|_K$ remain invariant under basis choice. The integer

certificate, scalar depth, and their transport properties complete the algebraic foundation for the curvature gate introduced next.

SNF certificate (sketch). $\Delta W_{\text{EM}} = \begin{bmatrix} 8 & 8 & 224 \\ 0 & 1 & 18 \end{bmatrix}$ has integer rank 2, so $\ker_{\mathbb{Z}}(\Delta W_{\text{EM}}) = \text{span}\{\pm \chi_{\text{EM}}\}$ with $\chi_{\text{EM}} = (-10, -18, 1)$ and $\Delta W_{\text{EM}} \chi_{\text{EM}} = 0$. Unimodular transport $M^T \chi_{\text{EM}} = \chi = (16, 13, 2)$ fixes the primitive generator, unique up to sign.

Even gate and definition of $G(x)$. Having identified the invariant scalar depth $\Xi = \chi \cdot \hat{\Psi}$, we introduce the curvature-response function (the *gate*) that modulates the emergent gravitational coupling. The gate must satisfy: (i) even parity about equilibrium [$\Pi'(\Xi_{\text{eq}}) = 0$]; (ii) analyticity and positivity for all Ξ ; (iii) normalization $\Pi(\Xi_{\text{eq}}) = 1$ (recovering GR at equilibrium); and (iv) minimal parameter freedom. A minimal analytic, even, and positive form meeting these is the Gaussian gate

$$\Pi(\Xi) = \exp\left[-\frac{(\Delta\Xi)^2}{\sigma_\chi^2}\right], \quad (4)$$

$$\Pi'(\Xi_{\text{eq}}) = 0, \quad \Pi(\Xi_{\text{eq}}) = 1, \quad (5)$$

which enforces parity-even curvature modulation and smooth suppression beyond the Planck-thin envelope ($|\Delta\Xi| \sim \sigma_\chi$). With $s_\Xi \equiv \Delta\Xi/\sigma_\chi$, $\phi_\chi \equiv \Delta\Xi/\|\chi\|_{\mathbf{K}_{\text{eq}}}$, $\Lambda_{\text{gate}} \equiv \sigma_\chi/\|\chi\|_{\mathbf{K}_{\text{eq}}}$, the laboratory null becomes $\frac{\Delta G}{G} = s_\Xi^2 = (\phi_\chi/\Lambda_{\text{gate}})^2$. The width σ_χ is fixed by Fisher curvature from SM covariance (pins at $\mu = M_Z$) [4, 5, 11], leaving no tunable parameters.

Gate parity. If Π is even and C^2 near Ξ_{eq} , then $\Pi'(\Xi_{\text{eq}}) = 0$ and $\Pi(\Xi_{\text{eq}} + \Delta\Xi) = 1 - (\Delta\Xi)^2/\sigma_\chi^2 + \mathcal{O}((\Delta\Xi)^4)$; any observed $\mathcal{O}((\Delta\Xi))$ term would falsify parity or alignment.

Write the laboratory template as

$$\frac{\Delta G}{G} = A s + B s^2 + \mathcal{O}(s^3), \quad s \equiv \frac{\Delta\Xi}{\sigma_\chi}.$$

For an even gate we expect $A = 0$ and $B = 1$. Equivalently, in the ϕ_χ normalization,

$$\frac{\Delta G}{G} = A' \phi_\chi + B' \phi_\chi^2 + \dots, \quad A' = 0, \quad B' = \frac{1}{\Lambda_{\text{gate}}^2}.$$

Any reproducible odd term ($A \neq 0$ or $A' \neq 0$) falsifies alignment parity.

Definition (natural units). In natural units ($\hbar = c = 1$), the Standard Model itself fixes the gravitational coupling:

$$G \equiv \frac{\Omega}{m_p^2}, \quad (6)$$

$$\Omega \equiv \hat{\alpha}_s^{16} \hat{\alpha}_2^{13} \hat{\alpha}^2, \quad (7)$$

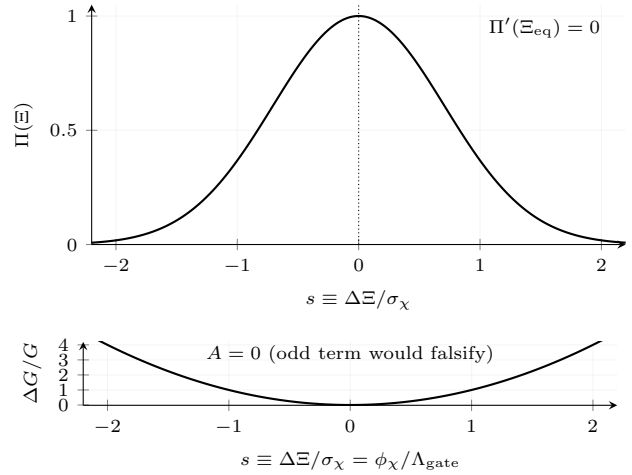


FIG. 1. Even gate $\Pi(\Xi) = \exp[-(\Delta\Xi)^2/\sigma_\chi^2]$ vs. $s = \Delta\Xi/\sigma_\chi$. $\Pi'(\Xi_{\text{eq}}) = 0$ enforces parity. Quadratic lab-null template $\Delta G/G = s^2/\Lambda_{\text{gate}}^2$; an odd term $A s$ would falsify alignment.

$$G(x) = G \Pi(\Xi(x)). \quad (8)$$

For SI units, restore the dimensional factor \hbar :

$$G = \frac{\Omega \hbar c}{m_p^2}.$$

$$\Omega = \hat{\alpha}_s^{16} \hat{\alpha}_2^{13} \hat{\alpha}^2$$

$$G = \frac{\Omega}{m_p^2}$$

$$\frac{G_* \Pi(\hat{\Xi})}{G_*} = \Pi(\hat{\Xi}) = \exp\left[-\frac{(\hat{\Xi} - \hat{\Xi}^{(\text{eq})})^2}{\sigma_\chi^2}\right]$$

Parity-even lab null and tensor sector. Even parity of the gate enforces a quadratic curvature response near equilibrium. With $\mathbf{K}_{\text{eq}} \succ 0$ and alignment of $\hat{\chi} = \chi / \|\chi\|_{\mathbf{K}_{\text{eq}}}$ to the soft eigenvector of \mathbf{K}_{eq} ,

$$\frac{\Delta G}{G} \simeq \frac{(\Delta\Xi)^2}{\sigma_\chi^2} = \frac{\phi_\chi^2}{\Lambda_{\text{gate}}^2}, \quad (9)$$

$$\phi_\chi = \frac{\chi^\top (\hat{\Psi} - \langle \hat{\Psi} \rangle)}{\|\chi\|_{\mathbf{K}_{\text{eq}}}}, \quad (10)$$

$$\Lambda_{\text{gate}} = \frac{\sigma_\chi}{\|\chi\|_{\mathbf{K}_{\text{eq}}}}. \quad (11)$$

This constitutes the *quadratic lab null*: any linear term in $\Delta G/G$ falsifies parity or alignment.

No $h-\phi$ mixing at linear order. $S \supset \frac{M_P^2}{2} \Pi(\Xi) R$. Since $\Pi'(\Xi_{\text{eq}}) = 0$, the variation $\delta\Omega = M_P^2 \Pi'(\Xi_{\text{eq}}) \delta\Xi$ vanishes, eliminating the $(g_{\mu\nu} \square - \nabla_\mu \nabla_\nu) \delta\Omega$ term at $\mathcal{O}(h)$. The remaining equation $\mathcal{E}_{\mu\nu}^{\alpha\beta} h_{\alpha\beta} = 0$ is the Lichnerowicz operator with $m_{\text{PF}} = 0$.

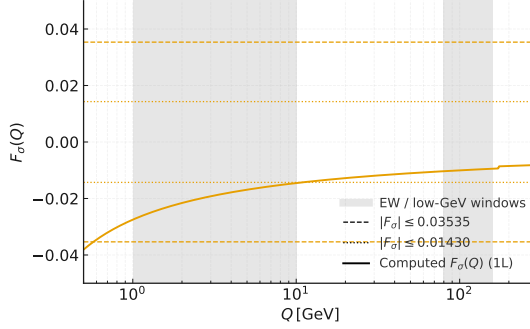


FIG. 2. Projected running $F(Q)$ within preregistered electroweak and low-GeV flatness windows (SM bounds and masks). Flatness corresponds to $\beta_\Xi = 0$ at one loop; mild threshold kinks appear outside the EW window.

Because $\Pi'(\Xi_{\text{eq}}) = 0$, the linearized equation reduces to

$$\Delta_L h_{\mu\nu} \equiv -\square h_{\mu\nu} = 0, \quad (12)$$

so the tensor mode is GR-normalized, massless, and luminal (helicity 2) [6, 7, 12, 13].

Pinned scales. With $K_{\text{eq}} \succ 0$, the gate scale is

$$\Lambda_{\text{gate}} = \frac{\sigma_\chi}{\|\chi\|_{K_{\text{eq}}}}.$$

From SM pins at $\mu = M_Z$ one finds $\sigma_\chi = 247.683$ and $\|\chi\|_{K_{\text{eq}}} = 17.6278$, giving $\Lambda_{\text{gate}} = 14.0507$ (full derivation in the Supplement).

TABLE I. Equilibrium kinetic metric K_{eq} : eigenvalues and alignment diagnostics.

Eigenvalues ($\lambda_1, \lambda_2, \lambda_3$)	$\ \chi\ _{K_{\text{eq}}}$	$\cos \theta_K$	$\varepsilon_{\text{align}}$
(0.7243, 2.0156, 3.2599)	17.6278	0.9999999998	$< 10^{-3}$

Running of G and Ward-flatness. Because G is composed of Standard Model couplings, its renormalization behavior follows theirs. Differentiating $\Xi = \chi \cdot \hat{\Psi}$ gives

$$\beta_\Xi \equiv \frac{d\Xi}{d\ln Q} = 16\frac{\beta_{\alpha_s}}{\alpha_s} + 13\frac{\beta_{\alpha_2}}{\alpha_2} + 2\frac{\beta_\alpha}{\alpha}, \quad (13)$$

$$\beta_\Xi = 0 \quad (\text{Ward-flat at one loop}). \quad (14)$$

Thus Ξ and G remain stationary at one loop, avoiding basis artifacts [1, 2]. Preregistered flatness windows and masks are evaluated in the SM; the figure shows $F(Q)$ remaining within those bounds.

Beyond equilibrium, slow variation of K_{eq} produces adiabatic tracking of the soft mode (dynamic alignment) and a small two-loop drift (quantified in the Supplement).

The running of G follows directly:

$$\beta_G \equiv \frac{d\ln G}{d\ln Q} = 16\frac{\beta_{\alpha_s}}{\alpha_s} + 13\frac{\beta_{\alpha_2}}{\alpha_2} + 2\frac{\beta_\alpha}{\alpha} = 0 + \mathcal{O}(\hat{\alpha}_i^2), \quad (15)$$

so G is flat at one loop with bounded higher-order drift [14]. Physically,

$$G(x) = G \Pi(\Xi(x)), \quad (16)$$

$$G = \frac{\Omega}{m_p^2}. \quad (17)$$

At $\mu = M_Z$ ($\overline{\text{MS}}$), comparison is made *a posteriori* to the metrological coupling $\alpha_G^{(\text{pp})}$ [15, 16].

Closure and prediction.

$$\Omega = \hat{\alpha}_s^{16} \hat{\alpha}_2^{13} \hat{\alpha}^2 \stackrel{?}{=} \alpha_G^{(\text{pp})} \equiv \frac{G_N m_p^2}{\hbar c}, \quad (18)$$

the *closure test* linking the Standard Model invariant to metrology [4, 11, 15, 16]. If equality holds within uncertainties,

$$G(\Xi_{\text{eq}}) = \frac{\Omega \hbar c}{m_p^2} = G_N.$$

Inverting gives the leave-one-out forecast

$$\hat{\alpha}_s^*(M_Z) = \left[\frac{\alpha_G^{(\text{pp})}}{\hat{\alpha}_2^{13} \hat{\alpha}^2} \right]^{1/16} = 0.1173411 \pm 1.86 \times 10^{-5}, \quad (19)$$

consistent with the PDG mean (-0.73σ) [4, 5]. The closure ratio

$$\frac{\Omega}{\alpha_G^{(\text{pp})}} = 1.09373393 \quad (+9.373\%)$$

serves as the empirical benchmark.

Matching (UV→IR). Define

$$G = \frac{\Omega \hbar c}{m_p^2}, \quad G_N \equiv Z_G G, \quad (20)$$

$$Z_G = \frac{\alpha_G^{(\text{pp})}}{\Omega} = 0.91430 \quad (-8.57\%), \quad (21)$$

which absorbs scheme, threshold, and higher-order effects (full budget in the Supplement).

Helicity scale. At equilibrium, the soft-mode alignment fixes the gate scale $\Lambda_{\text{gate}} = \sigma_\chi / \|\chi\|_{K_{\text{eq}}} = 14.05$, yielding a helicity frequency $\omega_{\text{hel}} = 1/\Lambda_{\text{gate}}$ and period $T_{\text{hel}} = 2\pi\Lambda_{\text{gate}} \simeq 88 t_P$. This *Planck-thin curvature envelope* defines the coherence length of the emergent tensor mode and bounds the quadratic response $\Delta G/G \simeq \phi_\chi^2 / \Lambda_{\text{gate}}^2$, as detailed in Sec. S8 of the Supplemental Material.

Falsifiers (any suffices). The construction is parameter-free; any single failure falsifies it:

1. **Non-unique integer certificate.** The Smith-normal-form must yield a unique primitive left-kernel generator $\chi = (16, 13, 2)$; any alternate integer solution of comparable norm breaks the projection symmetry [8–10].

- 2. Odd (linear) curvature response.** With $\Pi'(\Xi_{\text{eq}}) = 0$, a measured linear term As in $\Delta G/G = As + Bs^2 + \dots$ (where $s = \Delta\Xi/\sigma_\chi$) falsifies parity or alignment. *Example:* taking $s = 9$ from SM pins gives

$$\frac{\Delta G}{G} \simeq s^2 = \left(\frac{\phi_\chi}{\Lambda_{\text{gate}}} \right)^2 = 1.32 \times 10^{-3},$$

accessible to symmetric $\pm s$ clock or torsion tests; a fit consistent with $A = 0$ is required.

- 3. Tensor-sector anomaly.** Any Pauli–Fierz mass or non-luminal dispersion violates GR-normalized propagation of the linearized mode [7, 12, 13].
- 4. Metric instability or misalignment.** K_{eq} must remain positive definite ($K_{\text{eq}} \succ 0$) with $\cos\theta_K \simeq 1$; a negative eigenvalue or deviation beyond $\varepsilon_{\text{align}}$ signals ghost or locking failure.
- 5. Ward-flatness violation.** The projected flow β_Ξ must remain zero within preregistered EW and low-GeV masks; significant drift implies RG-scheme dependence or breakdown of the aligned projection [1, 2].
- 6. Closure or LOO failure.** Deviation of $\Omega/\alpha_G^{(\text{pp})}$ from unity beyond pinned uncertainties, or $\hat{\alpha}_s^*(M_Z)$ outside PDG bounds, falsifies identification of G as SM-derived [4, 5, 15, 16].

Implications. Gravity emerges as the parity-even curvature response of the Standard Model gauge sector, with $G(x) = G\Pi(\Xi(x))$ fixed entirely by $\{\hat{\alpha}_s, \hat{\alpha}_2, \hat{\alpha}\}$ at M_Z [4–6, 11]. Two direct signatures make the framework falsifiable: (i) the quadratic lab-null $\Delta G/G \simeq (\Delta\Xi/\sigma_\chi)^2$, and (ii) the closure ratio $\Omega/\alpha_G^{(\text{pp})} = 1.09373393$. Any observed odd-parity term or closure mismatch beyond pinned uncertainties would refute the construction [7, 12, 13].

Scope note. This Letter establishes a first-principles derivation of the gravitational coupling G and its empirical closure within the Standard Model. Dynamic tensor-sector extensions—including the helicity frequency,

Planck-thin envelope, drift law, and the conserved alignment current—are detailed in the Supplemental Material. All analytic derivations and pinned numerical checks are reproducible from the accompanying `GAGE_repo` package.

The author conducted this work independently and received no external funding. Appreciation is extended to the Particle Data Group (PDG), CODATA, Overleaf, Python, and OpenAI’s ChatGPT for providing open access tools, data, and computational resources that made this study possible, and to the many authors whose prior work established the foundations used herein.

-
- [1] S. Weinberg, *The Quantum Theory of Fields, Vol. 2: Modern Applications* (Cambridge University Press, Cambridge, UK, 1996).
 - [2] M. E. Peskin and D. V. Schroeder, *An Introduction to Quantum Field Theory* (Addison-Wesley, Reading, MA, 1995).
 - [3] P. Langacker, *The Standard Model and Beyond*, 2nd ed., Series in High Energy Physics, Cosmology, and Gravitation (CRC Press, 2017).
 - [4] S. Navas *et al.* (Particle Data Group), Phys. Rev. D **110**, 030001 (2024), and 2025 update.
 - [5] T. Dorigo and M. Tanabashi, in *Review of Particle Physics*, edited by Particle Data Group (Oxford University Press, 2025) p. 083C01, published in Prog. Theor. Exp. Phys. 2025 (8), 083C01.
 - [6] S. M. Carroll, *Spacetime and Geometry: An Introduction to General Relativity* (Addison-Wesley, 2004).
 - [7] C. M. Will, Living Rev. Relativ. **17**, 4 (2014).
 - [8] T. Appelquist and J. Carazzone, Phys. Rev. D **11**, 2856 (1975).
 - [9] R. Kannan and A. Bachem, SIAM J. Comput. **8**, 499 (1979).
 - [10] M. Newman, Linear Algebra Appl. **254**, 367 (1997).
 - [11] J. Erler *et al.*, in *Review of Particle Physics* (Particle Data Group, 2024).
 - [12] B. Bertotti, L. Iess, and P. Tortora, Nature **425**, 374 (2003).
 - [13] R. Abbott *et al.* (LIGO Scientific Collaboration and Virgo Collaboration and KAGRA Collaboration), Phys. Rev. D (2021), combined bound $m_g \leq 1.27 \times 10^{-23} \text{ eV}/c^2$ (90% C.L.), arXiv:2112.06861 [gr-qc].
 - [14] F. Jegerlehner, Nucl. Part. Phys. Proc. **303–305**, 1 (2018), see also arXiv:1705.00263.
 - [15] P. J. Mohr, D. B. Newell, B. N. Taylor, and E. Tiesinga, Rev. Mod. Phys. **97**, 025002 (2025).
 - [16] D. Robinson and P. A. Zyla, in *Review of Particle Physics* (Particle Data Group, 2024) topical review, revised 2024.

Supplemental Material for: Gauge-Aligned Graviton Emergence (GAGE)

Michael DeMasi DNP

October 28, 2025

S0. Notation, pins, and conventions

Provenance and sources. All numerical inputs, constants, and coupling data used herein are taken from established references. The Standard Model framework and renormalization conventions follow Weinberg^[1], Peskin–Schroeder^[2], and Langacker^[3]. Decoupling and integer-lattice methods follow Appelquist–Carazzone^[4], Kannan–Bachem^[5], and Newman^[6]. Numerical pins and covariance values are drawn from the Particle Data Group and CODATA^[7–10]. Gravitational and metrological comparisons reference Carroll^[11], Will^[12], Bertotti^[13], and Abbott *et al.* (LVK)^[14]. Running of couplings follows Jegerlehner^[15]. All calculations are performed within $\overline{\text{MS}}$ at $\mu = M_Z$, with no external data sources beyond these references.

Purpose. This Supplemental Material provides the derivations, numeric checks, and reproducibility details referenced in the Letter. It fixes all symbols, evaluation points, and unit conventions, and defines the error-propagation and covariance rules used in tables and figures.

Contents. Hatted couplings; $\mu = M_Z$; $\overline{\text{MS}}$ scheme; PDG/CODATA pins with uncertainties; unit policy; error-propagation rules; equilibrium metric K_{eq} and eigenvalues; Smith–normal–form certificate for χ ; Fisher-width derivation of σ_χ ; Ward-flatness masks; closure and leave-one-out tests; reproducibility script and checksum manifest.

Coordinates and logs Work in log-coupling space with hats denoting $\overline{\text{MS}}$ at $\mu = M_Z$:

$$\hat{\Psi} = (\ln \hat{\alpha}_s, \ln \hat{\alpha}_2, \ln \hat{\alpha}), \quad \chi = (16, 13, 2), \quad \hat{\Xi} = \chi \cdot \hat{\Psi}$$

and the SM-internal invariant

$$\Omega \equiv e^{\hat{\Xi}} = \hat{\alpha}_s^{16} \hat{\alpha}_2^{13} \hat{\alpha}^2.$$

All EFT derivations in this SM proceed in log space; metrology targets are used only later (S5) for closure/LOO validation, not as inputs.

Units policy (concise) **SM pins:** $\overline{\text{MS}}$ at $Q = M_Z$ (hats by default) (SM pins @ M_Z , $\overline{\text{MS}}$)

EFT derivations: natural units ($\hbar = c = 1$), with explicit $\hbar c$ only when mapping back to SI

Metrology targets: SI values (PDG/CODATA) used only in S5 for closure/LOO, never upstream

Gate and metric

$$\frac{G \Pi(\hat{\Xi})}{G} = \Pi(\hat{\Xi}) = \exp\left[-\frac{(\hat{\Xi} - \hat{\Xi}^{(\text{eq})})^2}{\sigma_\chi^2}\right], \quad \mathbf{K}_{\text{eq}} \succ 0, \quad \|\mathbf{v}\|_{\mathbf{K}_{\text{eq}}}^2 = \mathbf{v}^\top \mathbf{K}_{\text{eq}} \mathbf{v}$$

with $\hat{\Xi}^{(\text{eq})} = \hat{\Xi}|_{\mu=M_Z}$, gate width σ_χ , and gate scale $\Lambda_{\text{gate}} = \sigma_\chi / \|\chi\|_{\mathbf{K}_{\text{eq}}}$. Even parity ($\partial_\Xi \Pi|_{\hat{\Xi}^{(\text{eq})}} = 0$) enforces the quadratic lab-null

$$\frac{\Delta G}{G} \simeq \frac{\Delta \hat{\Xi}^2}{\sigma_\chi^2} \quad \text{with} \quad \Delta \hat{\Xi} = \hat{\Xi} - \hat{\Xi}^{(\text{eq})}.$$

Notation Summary. Located at end of the document. Core scheme/pin conventions follow PDG/CODATA; the Ward-flatness projector and the one-loop identity $\beta_{\Xi} = 0$ (PRL Eq. (14)) are used later in S5.

Equilibrium convention Pins are $\overline{\text{MS}}$ at $Q = M_Z$; we set $\Pi(\hat{\Psi}_{\text{eq}}) = 1$ so $G\Pi(\hat{\Xi})|_{\text{eq}} = G$. Any identification with metrology (e.g., $G \stackrel{?}{=} G_N$) is tested only in S5.

Pins and sources (SM pins @ $\mu = M_Z$; metrology targets in S5 only) Table 2 lists *inputs used in derivations* (SM pins); Table 3 lists *closure targets not used as inputs* (metrology). See PRL Table I and Secs. “Running of G and Ward-flatness”—“Closure and prediction” for definitions. SM pins and electroweak conventions follow PDG; SI targets follow CODATA.

Error propagation and correlations Unless stated, use linearized Gaussian propagation in vector form:

$$\text{Cov}(f) = J \text{Cov}(x) J^T, \quad J_{ai} = \partial_{x_i} f_a, \quad \delta f^2 = \nabla f^T \text{Cov}(x) \nabla f.$$

For logarithms,

$$\delta(\ln x) \simeq \frac{\delta x}{x}, \quad \text{Cov}(\ln x, \ln y) \simeq \frac{\text{Cov}(x, y)}{xy}.$$

Inputs and correlations Include PDG/CODATA covariances where provided (e.g., components entering the running of $\hat{\alpha}$ to M_Z). When unavailable, treat inputs as independent and propagate to derived quantities (e.g., $\hat{\alpha}_2 = \hat{\alpha}/\sin^2\hat{\theta}_W$) via the Jacobian above. All reported uncertainties are 1σ .

Log-space propagation Quantities defined in log coordinates (e.g., $\hat{\Psi}$, $\hat{\Xi}$) use the same rules; returns to linear variables use $\sigma(y) \approx y \sigma(\ln y)$.

Metrology (target-only) handling Closure/LOO covariance, metrology depths, and any optional cross-covariances are handled in S5. We do not use metrology in upstream derivations.

Cross-references and reproducibility Definitions of Ω , closure, and LOO appear in PRL Eqs. (7), (18), and (19). The SM mirrors the Letter: S1 (SNF certificate), S2 (alignment principle), S3 (gate and parity lemma), S4 (tensor sector / no PF mass), S5 (Ward-flatness), S6 (closure and LOO), S7 (environmental lab-null), S8 (helicity scales).

Versioning and reproducibility All pins in Tables 2, 3, 4, 5, and 6 are frozen to the cited PDG/CODATA releases and mirrored locally. Section S9 points to the Repo’s `pins.json` (SI; $\overline{\text{MS}}$ at $\mu = M_Z$) and build scripts that regenerate the S0 tables and figure data from source pins. The build is deterministic (no network); SHA-256 hashes are emitted for all artifacts, and any drift indicates a pin or version change. Monte Carlo confirmation of closure/LOO appears only in the SM (Sec. S6.8) and reproduces the linearized propagation. The Repo remains deterministic (no RNG) and regenerates numeric tables and figure data from pinned inputs only.

Reproduction (pointer to Repo) S9 summarizes inputs/outputs and checksums; the complete, executable workflow lives in the accompanying Repo document (source of truth). From the Repo:

- `pins.json` and `keq.json` (MS at $\mu = M_Z$); code derives $\hat{\alpha}_2 = \hat{\alpha}/\sin^2\hat{\theta}_W$
- one-command rebuild: `bash build.sh` (*or Windows build_win.bat*) → regenerates numeric tables and figure data from pins
- optional metrics: `src/metric_eigs.py` emits `metric_results.json` (K_{eq} eigs/evecs, $\|\chi\|_K$, Λ_{gate} , alignment)
- deterministic run; SHA-256 of all artifacts recorded in `SHA256SUMS.txt`

S9 records filenames, versions, and hashes matching the Repo; code listings are omitted here by design.

Vector form (Jacobian rule) For a vector map $y = f(x)$ with inputs $x = (x_1, \dots, x_n)$ and outputs $y = (y_1, \dots, y_m)$,

$$\text{Cov}(y) = J \text{Cov}(x) J^\top, \quad J_{ij} = \frac{\partial y_i}{\partial x_j}.$$

Log domain Define $\xi_i = \ln x_i$. For monomials $y = \prod_i x_i^{a_i}$,

$$\ln y = \sum_i a_i \xi_i, \quad \delta(\ln y)^2 = \sum_i a_i^2 \delta\xi_i^2 + 2 \sum_{i < j} a_i a_j \text{Cov}(\xi_i, \xi_j).$$

For small errors, $\delta(\ln x) \simeq \delta x/x$ and $\text{Cov}(\ln x, \ln y) \simeq \text{Cov}(x, y)/(xy)$.

Example (derived SU(2) coupling) With $\hat{\alpha}_2 = \hat{\alpha}/\sin^2\hat{\theta}_W$,

$$\ln \hat{\alpha}_2 = \ln \hat{\alpha} - \ln(\sin^2\hat{\theta}_W), \quad \sigma^2(\ln \hat{\alpha}_2) = \sigma^2(\ln \hat{\alpha}) + \sigma^2(\ln \sin^2\hat{\theta}_W) - 2 \text{Cov}(\ln \hat{\alpha}, \ln \sin^2\hat{\theta}_W),$$

and $\sigma(\hat{\alpha}_2) \approx \hat{\alpha}_2 \sigma(\ln \hat{\alpha}_2)$.

Derived inputs (closed forms used throughout) (i) **SU(2) coupling**

$$\hat{\alpha}_2 = \hat{\alpha}/\sin^2\hat{\theta}_W.$$

In linear variables (set $\text{Cov} = 0$ unless specified):

$$\delta\hat{\alpha}_2^2 = \left(\frac{1}{\sin^2\hat{\theta}_W}\right)^2 \delta\hat{\alpha}^2 + \left(\frac{\hat{\alpha}}{(\sin^2\hat{\theta}_W)^2}\right)^2 \delta(\sin^2\hat{\theta}_W)^2 - 2 \frac{\hat{\alpha}}{(\sin^2\hat{\theta}_W)^3} \text{Cov}(\hat{\alpha}, \sin^2\hat{\theta}_W).$$

Equivalently, in logs,

$$\delta \ln \hat{\alpha}_2^2 = \delta \ln \hat{\alpha}^2 + \delta \ln(\sin^2\hat{\theta}_W)^2 - 2 \text{Cov}(\ln \hat{\alpha}, \ln(\sin^2\hat{\theta}_W)), \quad \text{Cov}(\ln \hat{\alpha}, \ln \sin^2\hat{\theta}_W) \simeq \frac{\text{Cov}(\hat{\alpha}, \sin^2\hat{\theta}_W)}{\hat{\alpha} \sin^2\hat{\theta}_W}.$$

(ii) **Projection depth and certificate**

$$\hat{\Xi}^{(\text{eq})} = \chi \cdot (\ln \hat{\alpha}_s, \ln \hat{\alpha}_2, \ln \hat{\alpha}) = 16 \ln \hat{\alpha}_s + 13 \ln \hat{\alpha}_2 + 2 \ln \hat{\alpha}.$$

Work in the independent basis $x = (\ln \hat{\alpha}, \ln(\sin^2\hat{\theta}_W), \ln \hat{\alpha}_s)$ with $\ln \hat{\alpha}_2 = \ln \hat{\alpha} - \ln(\sin^2\hat{\theta}_W)$:

$$\hat{\Xi}^{(\text{eq})} = 15 \ln \hat{\alpha} - 13 \ln(\sin^2\hat{\theta}_W) + 16 \ln \hat{\alpha}_s, \quad g_\Xi = (15, -13, 16),$$

$$\sigma^2(\hat{\Xi}^{(\text{eq})}) = g_\Xi^\top \text{Cov}(x) g_\Xi, \quad \sigma(\Omega) \simeq \Omega \sigma(\hat{\Xi}^{(\text{eq})}).$$

(Use this x -basis again in S5 to avoid double counting.)

Ward-flatness prereg thresholds Define $F(Q) = d\hat{\Xi}/d\ln Q$ and the normalized monitor $F_\sigma(Q) = F(Q)/\sigma_\chi$ with masks around thresholds. The preregistered bounds are on F_σ :

EW [80, 160] GeV : $\|F_\sigma\|_\infty \leq 0.01430$, $\text{RMS}(F_\sigma) \leq 0.01372$, $|\langle F_\sigma \rangle| \leq 0.01372$,

Low-GeV [1, 10] GeV : $\|F_\sigma\|_\infty \leq 0.03535$, $\text{RMS}(F_\sigma) \leq 0.02622$, $|\langle F_\sigma \rangle| \leq 0.02585$.

Notes: Bounds are preregistered from the max across 1L/off and 2L/off runs with a $1.5\times$ inflation and include masked thresholds.

S1. Smith–Normal–Form (SNF) certificate for $\chi = (16, 13, 2)$

Goal Show that χ is fixed by integer structure alone (unique primitive generator up to sign), independent of masses, scales, or scheme choices within the admissible class.

Standing assumptions SM with three families and one Higgs doublet; GUT-normalized hypercharge ($\alpha_1 = \frac{5}{3}\alpha_Y$); mass-independent scheme with Appelquist–Carazzone decoupling. Fix a single $U(1)_Y$ integerization so that $U(1)$ weights are integers for each light set:

$$w_1^{(\text{f})} = 12 \sum_{\text{Weyl}} Y^2, \quad w_1^{(\text{s})} = 3 \sum_{\text{scalars}} Y^2.$$

For $H \sim (\mathbf{1}, \mathbf{2}, \frac{1}{2})$, $\sum Y^2 = 2 \times (\frac{1}{2})^2 = \frac{1}{2} \Rightarrow w_1(H) = 3$. The ordering of $(\hat{\alpha}_s, \hat{\alpha}_2, \hat{\alpha})$ is a notational convention; permutations simply relabel the components of χ while the kernel direction (and $\Xi = \chi^\top \Psi$) is basis-invariant.

S1.1 Construction recipe (per multiplet)

Per-multiplet weights and integerization. For each light multiplet f in an admissible window \mathcal{W} ,

$$\begin{aligned} \text{Weyl: } & w_3(f) = 4 T_{SU(3)}(f) d_{\text{spect}}(f), & w_2(f) = 4 T_{SU(2)}(f) d_{\text{spect}}(f), \\ \text{scalar: } & w_3(f) = 1 \cdot T_{SU(3)}(f) d_{\text{spect}}(f), & w_2(f) = 1 \cdot T_{SU(2)}(f) d_{\text{spect}}(f), \end{aligned}$$

and choose a single $U(1)_Y$ integerizer so the hypercharge column is integral:

$$w_1^{(\text{f})} = 12 \sum_{\text{Weyl in } f} Y^2, \quad w_1^{(\text{s})} = 3 \sum_{\text{scalars in } f} Y^2.$$

Here $T_{SU(N)}$ is the Dynkin index ($T(\mathbf{3}) = T(\mathbf{2}) = \frac{1}{2}$), and d_{spect} counts spectator multiplicities (e.g., color for $SU(2)$ weights and weak multiplicity for $SU(3)$ weights). GUT normalization is used for hypercharge: $\alpha_1 = \frac{5}{3}\alpha_Y$.

Window vectors and differences. Sum the weights across the light content of the window:

$$b^{(\mathcal{W})} = \begin{pmatrix} \sum_f w_3(f) \\ \sum_f w_2(f) \\ \sum_f w_1(f) \end{pmatrix} \in \mathbb{Z}^3,$$

then form the integer *difference stack* over admissible window pairs $\{(\mathcal{W}_i, \mathcal{W}_j)\}$:

$$\Delta b^{(ij)} = b^{(\mathcal{W}_i)} - b^{(\mathcal{W}_j)}, \quad \Delta W = \begin{bmatrix} (\Delta b^{(i_1 j_1)})^\top \\ (\Delta b^{(i_2 j_2)})^\top \\ \vdots \end{bmatrix} \in \mathbb{Z}^{m \times 3}.$$

Adjoint self-contributions cancel in Δb , exposing the rank-2 lattice used for SNF.

Sanity check (electromagnetic basis). After EWSB, use $w_{\text{EM}} = w_2 + \frac{5}{3}w_1 \Rightarrow 3w_{\text{EM}} = 3w_2 + 5w_1 \in \mathbb{Z}$, so the $(SU(3), SU(2), \text{EM})$ basis keeps exact integers for certification.

S1.2 Worked integer kernel (by hand, no SNF)

$$\chi_{\text{EM}} = (-10, -18, 1), \quad \gcd(10, 18, 1) = 1 \text{ (primitive).}$$

In the $(SU(3), SU(2), \text{EM})$ basis the two-row difference stack is

$$\Delta W_{\text{EM}} = \begin{bmatrix} 8 & 8 & 224 \\ 0 & 1 & 18 \end{bmatrix} \in \mathbb{Z}^{2 \times 3}.$$

Solve $\Delta W_{\text{EM}} \chi_{\text{EM}} = 0$ over \mathbb{Z} : second row gives $\chi_2 = -18\chi_3$; first row gives $8\chi_1 + 8\chi_2 + 224\chi_3 = 0 \Rightarrow 8\chi_1 + 8(-18)\chi_3 + 224\chi_3 = 0 \Rightarrow \chi_1 = -10\chi_3$. Choosing $\chi_3 = 1$ yields the *primitive* generator

$$\boxed{\chi_{\text{EM}} = (-10, -18, 1), \quad \gcd(10, 18, 1) = 1.}$$

Transport to the canonical basis Let $A \in \mathrm{GL}(3, \mathbb{Z})$ be the unimodular change-of-columns from the EM stack to the canonical (w_3, w_2, w_1) basis printed below. Kernel covectors transport contravariantly:

$$\boxed{\chi = A^{-\top} \chi_{\mathrm{EM}}}.$$

Evaluating with the A (denoted M below) gives

$$M^\top \chi_{\mathrm{EM}} = (16, 13, 2) \equiv \boldsymbol{\chi}.$$

SNF note The Smith invariants of ΔW_{EM} are $[1, 8]$ (rank 2), with a trailing zero column; hence $\ker_{\mathbb{Z}}(\Delta W_{\mathrm{EM}})$ is one-dimensional and generated by $\pm \chi_{\mathrm{EM}}$.

SNF (explicit). For $\Delta W_{\mathrm{EM}} = \begin{bmatrix} 1 & 1 & 28 \\ 0 & 1 & 18 \end{bmatrix}$, there exist unimodular $U \in GL(2, \mathbb{Z})$, $V \in GL(3, \mathbb{Z})$ such that

$$U \Delta W_{\mathrm{EM}} V = \mathrm{diag}(1, 8, 0),$$

so rank = 2 and there is a single zero invariant.

S1.3 Window differences and the integer row lattice

For a momentum window \mathcal{W} with light content $\mathcal{S}_{\mathcal{W}}$, define integerized 1L weights

$$b^{(\mathcal{W})} = \begin{pmatrix} \sum w_3 \\ \sum w_2 \\ \sum w_1 \end{pmatrix} \in \mathbb{Z}^3,$$

with Weyl $w_{3,2} = 4 T_{SU(3,2)} d_{\mathrm{spect}}$ and scalar $w_{3,2} = 1 \cdot T_{SU(3,2)} d_{\mathrm{spect}}$, and w_1 as above. For admissible windows $\{\mathcal{W}_i\}$ form differences

$$\Delta b^{(ij)} = b^{(\mathcal{W}_i)} - b^{(\mathcal{W}_j)}, \quad \Delta W = \begin{bmatrix} (\Delta b^{(i_1 j_1)})^\top \\ (\Delta b^{(i_2 j_2)})^\top \\ \vdots \end{bmatrix} \in \mathbb{Z}^{m \times 3}.$$

Lemma (row-lattice invariance). Any two admissible stacks $\Delta W, \Delta W'$ are related by unimodular row operations (adding/removing differences; reordering) and appending/canceling common adjoint self-terms. Hence their integer row lattices coincide and their left kernels over \mathbb{Z} are identical.

$$M = \begin{bmatrix} -5 & -3 & -2 \\ 2 & 1 & 1 \\ 2 & 1 & 0 \end{bmatrix}, \quad \det M = -1, \quad M^\top \chi_{\mathrm{EM}} = (16, 13, 2).$$

Proof sketch. Differences generate the same subgroup as absolute rows modulo a common reference. Appending/removing a difference corresponds to adding/removing an integer row; permutations and sign flips are unimodular. Common adjoint self-terms cancel in any row difference. \square

S1.4 Two physical differences (explicit tallies)

Using $T(\mathbf{3}) = T(\mathbf{2}) = \frac{1}{2}$ and spectator multiplicities (weak multiplicity as spectator for $SU(3)$ weights; color multiplicity as spectator for $SU(2)$ weights), the integerized one-loop weights sum as follows.

One SM generation (five Weyl multiplets).

$$SU(3): \quad w_3(Q_L) = 4 \cdot \frac{1}{2} \cdot 2 = 4, \quad w_3(u_R) = 4 \cdot \frac{1}{2} \cdot 1 = 2, \quad w_3(d_R) = 4 \cdot \frac{1}{2} \cdot 1 = 2 \\ \Rightarrow \sum w_3 = 8,$$

$$SU(2): \quad w_2(Q_L) = 4 \cdot \frac{1}{2} \cdot 3 = 6, \quad w_2(L_L) = 4 \cdot \frac{1}{2} \cdot 1 = 2 \Rightarrow \sum w_2 = 8,$$

$$U(1)_Y \text{ (global integerizer): } w_1 = 12 \sum_{\text{Weyl}} Y^2 = 12 \left[\frac{1}{6} + \frac{4}{3} + \frac{1}{3} + \frac{1}{2} + 1 \right] = 40.$$

Thus

$$\Delta b_{\text{gen}} = (8, 8, 40).$$

One Higgs doublet (complex scalar). With $Y = +1/2$ and two weak components,

$$w_2(H) = 1 \cdot \frac{1}{2} \cdot 1 = 1, \quad w_1(H) = 3 \sum_{\text{scalars}} Y^2 = 3 \cdot \frac{1}{2} = 3, \quad w_3(H) = 0,$$

so

$$\Delta b_H = (0, 1, 3).$$

(Any overall common integer factor on a *row* does not affect the *primitive* kernel.)

Conclusion (cross-check). The tally route (S1.4) and the EM-stack/SNF route yield the same primitive kernel $\chi = (16, 13, 2)$, closing the algebraic–physical loop and fixing χ by integer structure alone.

S2. Alignment as a Symmetry-Locking Principle

Statement. Let $\mathbf{K}_{\text{eq}} \succ 0$ be the equilibrium field-space metric and $\chi = (16, 13, 2)$ the SNF-certified projector. Define $\hat{\chi} = \chi / \|\chi\|_{\mathbf{K}_{\text{eq}}}$ and let e_{soft} be the normalized soft eigenvector of \mathbf{K}_{eq} . The *alignment condition* is

$$\cos \theta = \hat{\chi}^\top \mathbf{K}_{\text{eq}} e_{\text{soft}} \geq 1 - \varepsilon_{\text{align}},$$

with fixed tolerance $\varepsilon_{\text{align}} \ll 1$ (reported in SM). When alignment holds, the gauge–log depth $\hat{\Xi} = \chi \cdot \hat{\Psi}$ isolates the soft direction and the parity-even gate $\Pi(\hat{\Xi})$ projects the gauge sector onto a single scalar depth.

Consequences. (i) *Even-parity protection.* A spurion \mathbb{Z}_2 symmetry $\hat{\Xi} \rightarrow -\hat{\Xi}$ with Π invariant implies

$$\partial_{\Xi} \Pi(\hat{\Xi}) \Big|_{\hat{\Xi}(\text{eq})} = 0 \Rightarrow \text{no linear response; } m_{\text{PF}}^2 = 0,$$

to all loop orders near equilibrium. Renormalization can shift $(\sigma_\chi, \mathbf{K}_{\text{eq}})$ but cannot generate an odd term.

(ii) *Tensor sector.* Around the lab point (Minkowski) the Lichnerowicz operator reduces to

$$\Delta_L h_{\mu\nu} = -\square h_{\mu\nu} = 0 \Rightarrow \omega^2 = \mathbf{k}^2, \lambda = \pm 2 \text{ (massless, luminal)}.$$

(iii) *Quadratic lab-null.* The near-eq. response is

$$\frac{\Delta G}{G} \simeq \frac{\Delta \hat{\Xi}^2}{\sigma_\chi^2} = \frac{\varphi_\chi^2}{\Lambda_{\text{gate}}^2}, \quad \varphi_\chi = \Delta \hat{\Xi} / \|\chi\|_{\mathbf{K}_{\text{eq}}}, \quad \Lambda_{\text{gate}} = \sigma_\chi / \|\chi\|_{\mathbf{K}_{\text{eq}}}.$$

Falsifier from misalignment. If $\cos \theta < 1 - \varepsilon_{\text{align}}$, an odd (linear) term is generically induced in a lab fit

$$\frac{\Delta G}{G}(s) = A s + B s^2 + \dots,$$

violating the parity null ($A = 0$). Significant misalignment therefore falsifies the model.

Motivation (minimal). Alignment is the universal tendency of coupled fields to cohere along the softest kinetic mode of a positive-definite metric K . In GAGE, the certified integer projector χ aligns with the soft eigenvector of \mathbf{K}_{eq} , enforcing even response and a massless, luminal tensor sector. Analogous locking appears in magnetic ordering, superconductivity, and Higgs vacuum alignment (qualitative context; not inputs).

S2.1 Minimal alignment functional. Let unit order parameters $u_i(x) \in \mathbb{R}^d$ with metrics $K_i \succ 0$ and couplings γ_1, γ_2 . Define

$$\mathcal{A}[u] = \int d^D x \left[\frac{1}{2} \sum_i (\partial u_i)^\top K_i (\partial u_i) - \frac{1}{N} \sum_{i < j} (\gamma_1 u_i \cdot u_j + \gamma_2 (u_i \cdot u_j)^2) \right], \quad \|u_i\| = 1.$$

Diagnostics $m = \|\langle u \rangle\|$, $C = \frac{1}{N} \sum_i u_i u_i^\top$, and $\rho = \lambda_{\max}(C)/\text{Tr}(C)$ measure coherence ($m \in [0, 1]$, $\rho \in [1/d, 1]$).

Lemma. For $K \succ 0$ and couplings above a threshold γ_c , minimizers align $\langle u \rangle$ with the soft eigenvector e_{soft} of K up to $O(\kappa_{\text{gap}}^{-1})$; orthogonal fluctuations are gapped. **Map to GAGE.** $u \parallel \hat{\chi}$, $K \rightarrow \mathbf{K}_{\text{eq}}$, $\Xi = \chi \cdot \hat{\Psi}$, and even $\Pi(\Xi)$ enforces $\frac{\Delta G}{G} \simeq \varphi_\chi^2 / \Lambda_{\text{gate}}^2$.

S2.2 Phase variant (S¹). For phases θ_i ,

$$\mathcal{A}_\theta[\theta] = \int d^D x \left[\frac{\kappa}{2} \sum_i |\nabla \theta_i|^2 - \frac{K}{N} \sum_{i < j} \cos(\theta_i - \theta_j) \right],$$

whose ordered phase satisfies $\partial_\mu \theta_i \approx \partial_\mu \theta_j$, corresponding to alignment of phase gradients.

S2.3 Conservation form (near equilibrium). Define the alignment current

$$J_{\text{align}}^\mu = \Pi(\Xi) \chi^\top \mathbf{K}_{\text{eq}} \partial^\mu \hat{\Psi},$$

which reduces after one contraction to $J_{\text{align}}^\mu = \Pi(\Xi) \partial^\mu \Xi$. Using $\Pi'(\Xi_{\text{eq}}) = 0$ and the Ξ equation of motion,

$$\partial_\mu J_{\text{align}}^\mu = 0 + O((\Delta \hat{\Xi})^3, \text{two-loop drift}, \varepsilon_{\text{align}}).$$

Any measured odd term $A \neq 0$ in $\frac{\Delta G}{G} = A s + B s^2 + \dots$ gives $\partial_\mu J_{\text{align}}^\mu \neq 0$ and falsifies alignment.

S2.4 Information-geometry view. The Fisher curvature $\kappa_\chi = 1/\sigma_\chi^2$ defines the local informational metric. Alignment is motion along the soft eigenvector of \mathbf{K}_{eq} , the direction of least informational curvature.

S2.5 Falsifiers and caveats. Falsifiers include a persistent odd response ($A \neq 0$), failure of rank-1 coherence ($\rho \not\approx 1$), or alignment to a non-soft mode at fixed K . Boundary or disorder effects can produce modulated/defect states; diagnose via the most unstable Fourier mode of the quadratic expansion.

S2.6 Cross-domain statement. Across spins, phases, and gauge directions, alignment is symmetry locking to the soft mode of K , quantified by (m, ρ) . GAGE is the SM realization with $u \parallel \hat{\chi}$ and $K = \mathbf{K}_{\text{eq}}$.

S3. Gate, parity lemma, and quadratic response

S3.1 Even gate $\Pi(\Xi)$ and normalization

Promote $\hat{\Xi} = \chi \cdot \hat{\Psi}$ to a spacetime scalar $\hat{\Xi}(x)$ via $\hat{\Psi}(x)$. Define a parity-even projection gate

$$\frac{G \Pi(\hat{\Xi})}{G} = \Pi(\hat{\Xi}), \quad \Pi((\hat{\Xi}^{(\text{eq})}) = 1, \quad \Pi((\hat{\Xi}^{(\text{eq})} + \Delta) = \Pi((\hat{\Xi}^{(\text{eq})} - \Delta),$$

with Π assumed C^2 near $\hat{\Xi}^{(\text{eq})}$ and depending only on $\hat{\Xi}$. It introduces no gravitational dynamics beyond a multiplicative normalization.

Gaussian model (optional, for figures/tests) For numerical plots we sometimes use the Gaussian ansatz

$$\Pi_G(\Xi) = \exp\left[-\frac{(\Xi - \hat{\Xi}^{(eq)})^2}{\sigma_\chi^2}\right],$$

but all derivations require only evenness and smoothness.

S3.2 Parity lemma and quadratic response

Let $\Delta\hat{\Xi} \equiv \hat{\Xi} - \hat{\Xi}^{(eq)}$. Evenness implies $\partial_\Xi\Pi|_{\hat{\Xi}^{(eq)}} = 0$ and

$$\Pi((\hat{\Xi}^{(eq)} + \Delta\hat{\Xi})) = 1 + \frac{1}{2}\Pi'(\hat{\Xi}^{(eq)})\Delta\hat{\Xi}^2 + \mathcal{O}((\Delta\hat{\Xi})^3).$$

Hence

$$\frac{\Delta G}{G} = \frac{G\Pi(\hat{\Xi})}{G} - 1 = \Pi((\hat{\Xi}^{(eq)} + \Delta\hat{\Xi})) - 1 \simeq \frac{1}{2}\Pi'(\hat{\Xi}^{(eq)})\Delta\hat{\Xi}^2,$$

and all odd corrections vanish: $\partial_\Xi^{(2k+1)}\Pi|_{\hat{\Xi}^{(eq)}} = 0$. For Π_G , $\Pi''_G(\hat{\Xi}^{(eq)}) = -2/\sigma_\chi^2$, so $|\Delta G/G| \simeq \Delta\hat{\Xi}^2/\sigma_\chi^2$.

S3.3 Soft mode, canonical form, and $\Lambda_{\text{gate}} = \sigma_\chi/\|\chi\|_{\mathbf{K}_{\text{eq}}}$

With $\mathbf{K}_{\text{eq}} \succ 0$ (Table 5), define

$$\varphi_\chi = \frac{\chi^\top(\hat{\Psi} - \hat{\Psi}_{\text{eq}})}{\|\chi\|_{\mathbf{K}_{\text{eq}}}}, \quad \|\chi\|_{\mathbf{K}_{\text{eq}}} = \sqrt{\chi^\top \mathbf{K}_{\text{eq}} \chi},$$

so $\Delta\hat{\Xi} = \|\chi\|_{\mathbf{K}_{\text{eq}}} \varphi_\chi$. A convenient canonical parameterization is

$$\Pi(\hat{\Xi}) = \exp\left[-\frac{\varphi_\chi^2}{\Lambda_{\text{gate}}^2}\right], \quad \Lambda_{\text{gate}} = \frac{\sigma_\chi}{\|\chi\|_{\mathbf{K}_{\text{eq}}}},$$

and near equilibrium $|\Delta G/G| \simeq \varphi_\chi^2/\Lambda_{\text{gate}}^2$. The macros encode

$$\omega_{\text{hel}} = \frac{\|\chi\|_{\mathbf{K}_{\text{eq}}}}{\sigma_\chi} = \frac{1}{\Lambda_{\text{gate}}}, \quad T_{\text{hel}} = \frac{2\pi}{\omega_{\text{hel}}} = 2\pi\Lambda_{\text{gate}}.$$

S3.4 Spurion \mathbb{Z}_2 and radiative stability (all orders)

Definition (spurion parity). Assign the *spurionic* reflection symmetry in gauge-log space

$$\Xi \mapsto -\Xi, \quad \delta\Xi \mapsto -\delta\Xi, \quad \Pi \mapsto \Pi,$$

and act trivially on directions orthogonal to χ : $P_\perp(\hat{\Psi} - \hat{\Psi}_{\text{eq}}) \mapsto P_\perp(\hat{\Psi} - \hat{\Psi}_{\text{eq}})$ with $P_\perp = \mathbb{1} - P_\chi$ and $P_\chi = \mathbf{K}_{\text{eq}}\chi\chi^\top/(\chi^\top \mathbf{K}_{\text{eq}}\chi)$.

Lemma (operator classification near $\hat{\Xi}^{(eq)}$). In a local EFT respecting the spurion parity and the residual $O(2)$ rotations in the orthogonal complement, any scalar functional that multiplies the Ricci term must be built from *even* invariants:

$$\Pi(\Xi, \partial\Xi, \dots) = \Pi_0 + \Pi_2 \frac{\delta\Xi^2}{\sigma_\chi^2} + \Pi_{2,\partial} \frac{(\partial\delta\Xi)^2}{\Lambda_{\text{gate}}^2} + \dots,$$

while all terms linear in $\delta\Xi$ or odd in derivatives are forbidden.

Radiative stability (renormalization statement). Loop corrections consistent with the spurion parity cannot generate a linear term: $\partial_\Xi\Pi|_{\hat{\Xi}^{(eq)}}$ renormalizes multiplicatively to zero. Allowed counterterms renormalize (i) the overall normalization $\Pi(\hat{\Xi}^{(eq)}) \equiv 1$ (fixed by calibration), (ii) the width σ_χ , (iii) the kinetic metric K_{ij} , and higher-even coefficients. Hence the *only* effect at quadratic order is a finite renormalization of σ_χ and K_{ij} ; no $\mathcal{O}((\Delta\hat{\Xi})^2)$ response appears to any loop order.

S3.5 Why $\Pi = \Pi(\Xi)$ (no dependence on orthogonal modes)

By construction $\Xi = \chi \cdot \hat{\Psi}$ is the unique (primitive) integer depth (S1). Near equilibrium, the orthogonal subspace is two-dimensional; imposing the residual $O(2)$ symmetry in P_\perp forbids any dependence on a specific orthogonal direction at leading order. Therefore the most general scalar gate consistent with these symmetries is a function of Ξ alone (plus *even* derivative corrections as in S3.4), which are higher order in the lab-null setups of S6.

S3.6 Falsifier (boxed, S6 handoff)

$$\partial_\Xi \Pi(\Xi)|_{\hat{\Xi}^{(\text{eq})}} = 0 \implies \text{no linear term in } \frac{\Delta G}{G}. \text{ Any observed } \mathcal{O}(\Delta \hat{\Xi}) \text{ signal falsifies the construction.}$$

The quadratic coefficient is $\frac{1}{2} \Pi''(\hat{\Xi}^{(\text{eq})})$ (Gaussian: $-2/\sigma_\chi^2$). The lab-null template and two-state contrast appear in S6.

Parity reminder. At $\hat{\Psi}_{\text{eq}}$, $\partial_\Xi \Pi|_{\text{eq}} = 0$; hence no linear (odd) term in $\delta\Xi$ appears and leading deviations are $\propto \delta\Xi^2$.

S4. Tensor sector and absence of Pauli–Fierz mass

S4.1 Background, Jordan-frame expansion, and kinetic structure

Assume a stationary, flat laboratory background

$$\hat{\Psi} = \hat{\Psi}_{\text{eq}}, \quad \partial_{\hat{\Psi}} V|_{\hat{\Psi}_{\text{eq}}} = 0, \quad V(\hat{\Psi}_{\text{eq}}) = 0, \quad g_{\mu\nu} = \eta_{\mu\nu} + h_{\mu\nu}.$$

Insert the gate into the Einstein–Hilbert term:

$$S = \int d^4x \sqrt{-g} \left[\frac{1}{2} M_P^2 \Pi(\hat{\Xi}) R - \frac{1}{2} \partial_\mu \hat{\Psi}^\top \mathbf{K}(\hat{\Psi}) \partial^\mu \hat{\Psi} - V(\hat{\Psi}) \right].$$

At equilibrium $\Pi(\hat{\Xi}^{(\text{eq})}) = 1$ and, by S2, $\partial_\Xi \Pi(\Xi)|_{\hat{\Xi}^{(\text{eq})}} = 0$. Expand around $g_{\mu\nu} = \eta_{\mu\nu} + h_{\mu\nu}$ in harmonic gauge $\partial^\mu h_{\mu\nu} - \frac{1}{2} \partial_\nu h = 0$. To quadratic order in h ,

$$S_{\text{tens}}^{(2)} = \frac{M_P^2}{8} \int d^4x h^{\mu\nu} \mathcal{E}_{\mu\nu}^{\alpha\beta} h_{\alpha\beta} + \mathcal{O}(h^2 \Delta \hat{\Xi}^2),$$

where \mathcal{E} is the Lichnerowicz operator. Since $\Pi'(\hat{\Xi}^{(\text{eq})}) = 0$, all potential $h^2 \Delta \hat{\Xi}$ mixings vanish.

No Pauli–Fierz mass. Around flat equilibrium with $\Pi'(\hat{\Xi}^{(\text{eq})}) = 0$ and $\Pi(\hat{\Xi}^{(\text{eq})}) = 1$, the linearized tensor sector equals GR’s: no $m_{\text{PF}}^2(h_{\mu\nu} h^{\mu\nu} - h^2)$ term appears. Gate effects begin at $\mathcal{O}((\Delta \hat{\Xi}^2))$ and do not alter the kinetic Lichnerowicz form.

Kinetic metric and soft-mode projectors The log-coupling fields expand with

$$\mathcal{L}_{\text{kin}} = -\frac{1}{2} \partial_\mu \hat{\Psi}^\top \mathbf{K}(\hat{\Psi}) \partial^\mu \hat{\Psi}, \quad \mathbf{K}_{\text{eq}} = \mathbf{K}(\hat{\Psi})|_{\hat{\Psi}_{\text{eq}}} \succ 0.$$

Define the \mathbf{K}_{eq} -unit vector and projectors

$$\hat{u}_\chi = \frac{\boldsymbol{\chi}}{\|\boldsymbol{\chi}\|_{\mathbf{K}_{\text{eq}}}}, \quad P_\chi = \hat{u}_\chi \hat{u}_\chi^\top \mathbf{K}_{\text{eq}}, \quad P_\perp = \mathbb{1} - P_\chi,$$

so $\varphi_\chi = \hat{u}_\chi^\top \mathbf{K}_{\text{eq}}(\hat{\Psi} - \hat{\Psi}_{\text{eq}})$, and $\Delta \hat{\Xi} = \boldsymbol{\chi} \cdot (\hat{\Psi} - \hat{\Psi}_{\text{eq}}) = \|\boldsymbol{\chi}\|_{\mathbf{K}_{\text{eq}}} \varphi_\chi$. The explicit \mathbf{K}_{eq} and eigenstructure appear in Tables 5–6.

S4.2 Explicit origin of the no-mixing result

Vary the Jordan-frame Ricci term with $\Omega(\hat{\Psi}) \equiv M_P^2 \Pi(\Xi)$:

$$\delta(\sqrt{-g} \Omega R) = \sqrt{-g} \left[\frac{1}{2} \Omega h^{\mu\nu} \mathcal{E}_{\mu\nu}^{\alpha\beta} h_{\alpha\beta} + (g_{\mu\nu} \square - \nabla_\mu \nabla_\nu) \delta\Omega h^{\mu\nu} \right]_{\text{lin}} + \dots$$

Near equilibrium, $\delta\Omega = M_P^2 \Pi'(\hat{\Xi}^{(\text{eq})}) \delta\Xi + \mathcal{O}((\delta\Xi)^2) = 0 + \mathcal{O}((\delta\Xi)^2)$, so the would-be h $\delta\Xi$ mixing proportional to $(\partial\partial\delta\Omega)$ is absent at linear order. The first nonzero gate correction is $\mathcal{O}(h\delta\Xi^2)$, which cannot produce a Pauli–Fierz mass term and instead renormalizes higher-order interactions.

S4.3 GR limit and field equations (linearized)

Collect the $\mathcal{O}((h))$ terms and couple to conserved matter $T_{\mu\nu}$:

$$M_P^2 \mathcal{E}_{\mu\nu}^{\alpha\beta} h_{\alpha\beta} = T_{\mu\nu} + \mathcal{O}((h\delta\Xi^2)).$$

The gauge symmetries and propagator match GR; the two tensor polarizations propagate luminally with $k^2 = 0$. The Newtonian potentials satisfy

$$\nabla^2 \Phi = \nabla^2 \Psi = \frac{1}{2} M_P^{-2} T_{00} \Rightarrow \gamma \equiv \Psi/\Phi = 1 + \mathcal{O}((\Delta\hat{\Xi}^2/\sigma_\chi^2)),$$

consistent with the parity lemma (S2): odd response is forbidden and leading deviations are quadratic.

S4.4 Even scalar sector and width provenance

To parameterize widths without inducing a PF mass, use a parity-even quadratic potential in field space:

$$V(\hat{\Psi}) = \frac{1}{2} (\hat{\Psi} - \hat{\Psi}_{\text{eq}})^\top \Sigma_\perp^{-1} P_\perp (\hat{\Psi} - \hat{\Psi}_{\text{eq}}) + \frac{\gamma}{2} (\boldsymbol{\chi} \cdot (\hat{\Psi} - \hat{\Psi}_{\text{eq}}))^2,$$

with $\Sigma_\perp^{-1} \succ 0$ on P_\perp and $\gamma > 0$. The Hessian at equilibrium is

$$H \equiv \partial_i \partial_j V \Big|_{\text{eq}} = \Sigma_\perp^{-1} P_\perp + \gamma \boldsymbol{\chi} \boldsymbol{\chi}^\top.$$

The canonically normalized soft-mode mass is

$$m_\chi^2 = \frac{\boldsymbol{\chi}^\top H \boldsymbol{\chi}}{\boldsymbol{\chi}^\top \mathbf{K}_{\text{eq}} \boldsymbol{\chi}} = \frac{\boldsymbol{\chi}^\top \Sigma_\perp^{-1} P_\perp \boldsymbol{\chi}}{\boldsymbol{\chi}^\top \mathbf{K}_{\text{eq}} \boldsymbol{\chi}} + \gamma \frac{(\boldsymbol{\chi}^\top \boldsymbol{\chi})^2}{\boldsymbol{\chi}^\top \mathbf{K}_{\text{eq}} \boldsymbol{\chi}}.$$

Since $P_\perp \boldsymbol{\chi} = 0$,

$$m_\chi^2 = \gamma \frac{(\boldsymbol{\chi}^\top \boldsymbol{\chi})^2}{\boldsymbol{\chi}^\top \mathbf{K}_{\text{eq}} \boldsymbol{\chi}} \equiv \gamma_\chi \|\boldsymbol{\chi}\|_{\mathbf{K}_{\text{eq}}}^{-2}, \quad \gamma_\chi \equiv \gamma (\boldsymbol{\chi}^\top \boldsymbol{\chi})^2.$$

An even scalar potential thus produces widths in the scalar sector while preserving the massless, luminal spin-2 sector and forbidding any linear h - $\delta\Xi$ mixing.

S4.5 Covariant embedding (summary and cross-ref)

With

$$S = \int \sqrt{-g} \left[\frac{1}{2} \Omega(\hat{\Psi}) R - \frac{1}{2} G_{ij}(\hat{\Psi}) \nabla_\mu \xi^i \nabla^\mu \xi^j - V(\hat{\Psi}) + L_{\text{gauge}} + L_{\text{matter}} \right],$$

metric variation yields

$$\Omega G_{\mu\nu} + (g_{\mu\nu} \square - \nabla_\mu \nabla_\nu) \Omega = T_{\mu\nu}^{(\Psi)} + T_{\mu\nu}^{\text{gauge}} + T_{\mu\nu}^{\text{matter}}.$$

Calibrating $\Omega(\hat{\Psi}_{\text{eq}}) = M_P^2$ (i.e., $\Pi(\hat{\Xi}^{(\text{eq})}) = 1$) and using $\Pi'(\hat{\Xi}^{(\text{eq})}) = 0$ gives the GR quadratic sector exactly; expanding in $\delta\Xi$ reproduces the quadratic response of S3 with leading deviation $\Delta G/G \simeq \Delta\hat{\Xi}^2/\sigma_\chi^2$.

S4.6 Equilibrium metric and spectrum

Kinetic term (equilibrium metric) Work in log-coupling coordinates

$$\hat{\Psi} = (\hat{\xi}_s, \hat{\xi}_2, \hat{\xi}_\alpha) = (\ln \hat{\alpha}_s, \ln \hat{\alpha}_2, \ln \hat{\alpha}), \quad \hat{\Xi} = \chi \cdot \hat{\Psi}, \quad \chi = (16, 13, 2).$$

The scalar kinetic Lagrangian is

$$\boxed{\mathcal{L}_{\text{kin}} = -\frac{1}{2} \partial_\mu \hat{\Psi}^\top \mathbf{K}(\hat{\Psi})(\hat{\Psi}) \partial^\mu \hat{\Psi}, \quad \mathbf{K}(\hat{\Psi})(\hat{\Psi}) \succ 0} \quad (1)$$

and at the equilibrium point

$$\mathbf{K}_{\text{eq}} \equiv \mathbf{K}(\hat{\Psi})(\hat{\Psi}_{\text{eq}}) = \begin{bmatrix} 1.2509 & -0.6202 & -0.1813 \\ -0.6202 & 1.5128 & -0.1633 \\ -0.1813 & -0.1633 & 3.2362 \end{bmatrix}, \quad \mathbf{K}_{\text{eq}} \succ 0. \quad (2)$$

Spectrum and alignment Let $\{\lambda_i, e_i\}$ be the orthonormal eigenpairs of \mathbf{K}_{eq} (Euclidean inner product):

$$\lambda_{\min} = 0.7243366, \quad \lambda_2 = 2.0155976, \quad \lambda_{\max} = 3.2599658,$$

with

$$e_{\text{soft}} = (0.7724942, 0.6276375, 0.0965604), \quad \mathbf{K}_{\text{eq}} = \sum_{i=1}^3 \lambda_i e_i e_i^\top.$$

Numerically,

$$\hat{\chi} \equiv \frac{\chi}{\|\chi\|_2} = (0.7724873, 0.6276459, 0.0965609), \quad \cos \theta_{\mathbf{K}_{\text{eq}}} := \hat{\chi} \cdot e_{\text{soft}} = 1.0000000 \pm \mathcal{O}(10^{-8}),$$

and

$$\mathbf{K}_{\text{eq}} \chi = \lambda_{\min} \chi \pm \mathcal{O}(10^{-4}) \quad (\text{componentwise}).$$

Thus χ aligns with the soft eigenmode within numerical precision.

Metric-aware projectors (canonical)

$$\boxed{P_\chi = \frac{\chi \chi^\top \mathbf{K}_{\text{eq}}}{\chi^\top \mathbf{K}_{\text{eq}} \chi}, \quad P_\perp = \mathbb{1} - P_\chi} \quad (3)$$

Consequences (used throughout)

- **Depth norm:** $\|\chi\|_{\mathbf{K}_{\text{eq}}}^2 = \chi^\top \mathbf{K}_{\text{eq}} \chi = \lambda_{\min} \chi^\top \chi = \lambda_{\min} \times 429 \Rightarrow \|\chi\|_{\mathbf{K}_{\text{eq}}} = 17.6278$.
- **Gate scale:** with even curvature-gate width $\sigma_\chi = 247.683$, $\Lambda_{\text{gate}} = \sigma_\chi / \|\chi\|_{\mathbf{K}_{\text{eq}}} = 14.0507$, $\omega_{\text{hel}} = \Lambda_{\text{gate}}^{-1} = 0.0712$, $T_{\text{hel}} = 2\pi \Lambda_{\text{gate}} \simeq 88 t_P$.
- **Softest direction:** for any displacement ω , the quadratic form $Q(\omega) = \omega^\top \mathbf{K}_{\text{eq}} \omega$ is minimized along the χ direction; orthogonal motion costs more.

Eigen-decomposition and positivity Let $R = [e_1 \ e_2 \ e_3]$ be orthogonal. Then

$$R^\top \mathbf{K}_{\text{eq}} R = \text{diag}(\lambda_1, \lambda_2, \lambda_3), \quad \lambda_i > 0. \quad (4)$$

Depth direction and \mathbf{K}_{eq} norm For $\chi = (16, 13, 2)$, define

$$\|\chi\|_{\mathbf{K}_{\text{eq}}}^2 := \chi^\top \mathbf{K}_{\text{eq}} \chi, \quad \hat{\chi}_{\mathbf{K}_{\text{eq}}} := \frac{\chi}{\sqrt{\chi^\top \mathbf{K}_{\text{eq}} \chi}}, \quad \hat{\chi} := \frac{\chi}{\|\chi\|_2}. \quad (5)$$

(The alternative $\mathbf{K}_{\text{eq}} \chi \chi^\top / (\chi^\top \mathbf{K}_{\text{eq}} \chi)$ sometimes seen in the literature is *not* the \mathbf{K}_{eq} -orthogonal projector on column vectors.)

S4.7 Scalar potential, widths, and consistency certificate

Purpose The scalar potential below is not required for graviton emergence or GR normalization (those follow from the parity of the curvature gate $\Pi(\Xi)$; see S2/S3.2). This section only certifies that one can assign a consistent EFT width to the depth mode and regulate transverse directions without inducing a Pauli–Fierz mass or linear mixing.

Scalar potential (parity-even, quadratic) In log-coupling space write

$$\hat{\Psi} = (\hat{\xi}_s, \hat{\xi}_2, \hat{\xi}_\alpha) = (\ln \hat{\alpha}_s, \ln \hat{\alpha}_2, \ln \hat{\alpha}), \quad \chi = (16, 13, 2), \quad \hat{\Xi} = \chi \cdot \hat{\Psi},$$

and define $\Delta\hat{\Psi} = \hat{\Psi} - \hat{\Psi}_{\text{eq}}$, $\hat{\Xi}^{(\text{eq})} = \chi \cdot \hat{\Psi}_{\text{eq}}$. Take

$$V(\hat{\Psi}) = \frac{1}{2} \sum_{i \in \{s, 2, e\}} \frac{(\xi_i - \xi_i^{(\text{eq})})^2}{\sigma_i^2} + \frac{\gamma}{2} (\chi \cdot \Delta\hat{\Psi})^2, \quad (6)$$

so parity about $\hat{\Xi}^{(\text{eq})}$ is manifest: $\partial_{\xi_i} V|_{\text{eq}} = 0$ and all odd powers in $(\chi \cdot \Delta\hat{\Psi})$ vanish.

Equivalent projector/operator form (metric-correct) Let

$$P_\chi = \frac{\chi \chi^\top \mathbf{K}_{\text{eq}}}{\chi^\top \mathbf{K}_{\text{eq}} \chi}, \quad P_\perp = \mathbb{1} - P_\chi, \quad \mathbf{K}_{\text{eq}} \succ 0.$$

Then an equivalent form that makes the transverse restriction explicit is

$$V(\hat{\Psi}) = \frac{1}{2} \Delta\hat{\Psi}^\top (P_\perp \Sigma_\perp^{-1} P_\perp) \Delta\hat{\Psi} + \frac{\gamma}{2} (\chi \cdot \Delta\hat{\Psi})^2, \quad \Sigma_\perp^{-1} = \text{diag}\left(\frac{1}{\sigma_{\alpha_s}^2}, \frac{1}{\sigma_{\alpha_2}^2}, \frac{1}{\sigma_\alpha^2}\right). \quad (7)$$

(Using $P_\perp = \mathbb{1} - \mathbf{K}_{\text{eq}} \chi \chi^\top / (\chi^\top \mathbf{K}_{\text{eq}} \chi)$ would *not* be the \mathbf{K}_{eq} -orthogonal projector on column vectors; the form above is the correct one.)

Parameter choices (depth vs transverse) Depth (derived, fixed). From Tables 5 and 4:

$$\sigma_\chi = 247.683, \quad \|\chi\|_{\mathbf{K}_{\text{eq}}} = 17.6278, \quad \Lambda_{\text{gate}} = \frac{\sigma_\chi}{\|\chi\|_{\mathbf{K}_{\text{eq}}}} = 14.0507, \quad \omega_{\text{hel}} = \Lambda_{\text{gate}}^{-1} = 0.0712, \quad T_{\text{hel}} = 2\pi \Lambda_{\text{gate}} \simeq 88 t_P.$$

These follow from the Fisher curvature (gate width) and the kinetic norm.

Transverse (regulator pins, fixed once). The transverse widths regulate only the P_\perp plane:

$$\sigma_{\alpha_s} = 0.446296, \quad \sigma_{\alpha_2} = 0.547533, \quad \sigma_\alpha = 0.551281.$$

They do not affect the GR tensor sector (which depends only on gate parity; see S2/S3.2).

Isotropic fallback (metric-aware). If a symbolic fallback is desired, impose isotropy in the \mathbf{K}_{eq} -metric subspace orthogonal to χ :

$$\Sigma_\perp = C P_\perp, \quad P_\perp = \mathbb{1} - \frac{\chi \chi^\top \mathbf{K}_{\text{eq}}}{\chi^\top \mathbf{K}_{\text{eq}} \chi}$$

i.e., equal variance in any direction orthogonal to χ . (Componentwise recipes like $\sigma_i \propto |\chi_i|$ are not isotropic in the \mathbf{K}_{eq} metric and should be avoided.)

Hessian and depth-mode mass Expanding (7),

$$H \equiv \partial_i \partial_j V|_{\text{eq}} = P_\perp \Sigma_\perp^{-1} P_\perp + \gamma \chi \chi^\top. \quad (8)$$

Project along χ and normalize by $\mathbf{K}_{\text{eq}} \succ 0$:

$$m_\chi^2 = \frac{\chi^\top H \chi}{\chi^\top \mathbf{K}_{\text{eq}} \chi} = \frac{\chi^\top P_\perp \Sigma_\perp^{-1} P_\perp \chi}{\chi^\top \mathbf{K}_{\text{eq}} \chi} + \gamma \frac{(\chi^\top \chi)^2}{\chi^\top \mathbf{K}_{\text{eq}} \chi}. \quad (9)$$

Since $P_\perp \chi = 0$ by construction, the soft mass reduces to the depth-only certificate

$$m_\chi^2 = \gamma \frac{(\chi^\top \chi)^2}{\chi^\top \mathbf{K}_{\text{eq}} \chi} = \gamma_\chi \|\chi\|_{\mathbf{K}_{\text{eq}}}^{-2}, \quad \gamma_\chi \equiv \gamma(\chi^\top \chi)^2, \quad (10)$$

i.e. curvature resides only along the χ direction.

Transverse regulator implementation With the \mathbf{K}_{eq} -metric projectors above, implement the regulator as $P_\perp \Sigma_\perp^{-1} P_\perp$. This leaves the depth gate and tensor sector unchanged and avoids spurious mixing.

Gate in canonical form and parity lemma (recap) Define

$$\varphi_\chi = \frac{\chi^\top (\hat{\Psi} - \hat{\Psi}_{\text{eq}})}{\|\chi\|_{\mathbf{K}_{\text{eq}}}}, \quad \Delta \hat{\Xi} = \|\chi\|_{\mathbf{K}_{\text{eq}}} \varphi_\chi,$$

so

$$\Pi(\Xi) = \exp \left[-\frac{\varphi_\chi^2}{\Lambda_{\text{gate}}^2} \right], \quad \Lambda_{\text{gate}} = \frac{\sigma_\chi}{\|\chi\|_{\mathbf{K}_{\text{eq}}}}, \quad (11)$$

and near equilibrium $|\Delta G/G| \simeq \varphi_\chi^2/\Lambda_{\text{gate}}^2$ with the odd (linear) term absent: $\partial_\Xi \Pi|_{\hat{\Xi}(\text{eq})} = 0 \Rightarrow$ no $h\varphi$ linear mixing, no Pauli–Fierz mass.

Expansion about equilibrium and quadratic Lagrangian Set $\hat{\Psi} = \hat{\Psi}_{\text{eq}} + \varphi$ and $g_{\mu\nu} = \eta_{\mu\nu} + h_{\mu\nu}$. With $M_*^2 := M_P^2 \Pi(\Xi)|_{\hat{\Psi}=\hat{\Psi}_{\text{eq}}} = M_P^2$ and $\Delta \hat{\Xi} = \chi \cdot \varphi$,

$$\Pi(\Xi) = 1 - \Delta \hat{\Xi}^2 / \sigma_\chi^2 + \mathcal{O}((\varphi^4)).$$

To quadratic order,

$$\mathcal{L}^{(2)} = \frac{M_*^2}{8} h^{\mu\nu} \mathcal{E}_{\mu\nu}^{\rho\sigma} h_{\rho\sigma} - \frac{1}{2} \partial_\mu \varphi^\top \mathbf{K}_{\text{eq}} \partial^\mu \varphi - \frac{1}{2} \varphi^\top M^2 \varphi + \mathcal{O}(h^2 \varphi^2) + \mathcal{O}(h^2 \varphi), \quad (12)$$

with $M^2 = P_\perp \Sigma_\perp^{-1} P_\perp + \gamma \chi \chi^\top$ and \mathcal{E} the Lichnerowicz operator. By parity, linear $h\varphi$ mixing cancels and the graviton is massless and luminal.

Weinberg soft factor (unchanged) In the $q \rightarrow 0$ limit,

$$\mathcal{M}_{n+1} \simeq \kappa S^{(0)}(q, \varepsilon) \mathcal{M}_n, \quad S^{(0)} = \sum_{i=1}^n \eta_i \frac{p_i^\mu p_i^\nu \varepsilon_{\mu\nu}}{p_i \cdot q}, \quad \kappa = \frac{2}{M_*},$$

$\eta_i = \pm 1$, and $\varepsilon_{\mu\nu}$ is transverse and traceless. Depth parity at the lab point leaves $S^{(0)}$ invariant.

Light deflection Because $\Pi(\Xi) = 1 + \mathcal{O}((\Delta \hat{\Xi})^2)$, the leading eikonal angle is the GR value

$$\theta = \frac{4G M}{b c^2},$$

with fractional corrections $\mathcal{O}((\Delta \hat{\Xi}/\sigma_\chi)^2)$; in PPN language $\gamma_{\text{PPN}} = 1 + \mathcal{O}((\Delta \hat{\Xi}/\sigma_\chi)^2)$. (At equilibrium, $G=G_N$ by calibration.)

One-loop counterterm container map (near equilibrium) Divergences renormalize only $\{\Pi(\Xi), \mathbf{K}_{\text{eq}}, V(\hat{\Psi})\}$ and higher curvature. No linear $\Delta \hat{\Xi}$ counterterm appears by parity. Finite parts are absorbed as:

Positivity and bounds Working near equilibrium with diagonal tensor and regulated scalar sectors, require

$$\mathbf{K}_{\text{eq}} \succ 0, \quad \sigma_\chi^2 > 0, \quad \gamma > 0, \quad M_*^2 = M_P^2 \Pi(\hat{\Xi}^{(\text{eq})}) > 0,$$

ensuring GR tensor propagation and a stable scalar sector with no linear fifth force.

S5. RG running and Ward-flatness monitor

S5.1 Definition and admissible windows

Running-depth observable. In the $\overline{\text{MS}}$ scheme define

$$F(Q) \equiv \beta_{\Xi}(Q) = \boldsymbol{\chi} \cdot \frac{d\hat{\Psi}}{d\ln Q} = 16 \frac{d(\ln \hat{\alpha}_s)}{d\ln Q} + 13 \frac{d(\ln \hat{\alpha}_2)}{d\ln Q} + 2 \frac{d(\ln \hat{\alpha})}{d\ln Q}, \quad (13)$$

with $\hat{\Psi} = (\ln \hat{\alpha}_s, \ln \hat{\alpha}_2, \ln \hat{\alpha})$ and $\boldsymbol{\chi} = (16, 13, 2)$.

Admissible windows. A window \mathcal{W} is admissible if the particle content is fixed (mass-independent scheme), all heavy thresholds lie outside \mathcal{W} , and the EM basis is used post-EWSB. Within any such \mathcal{W} , Appelquist–Carazzone decoupling applies and the Smith–normal–form identity

$$\boldsymbol{\chi} \cdot b^{(\mathcal{W})} = 0 \quad (\text{one loop, GUT normalization}) \quad (14)$$

cancels the α -independent one-loop drift. Writing

$$F^{(1L)}(Q) = \frac{1}{2\pi} \sum_{i=1}^3 \chi_i b_i \alpha_i(Q), \quad (15)$$

the coupling weights $\alpha_i(Q)$ prevent an exact zero away from the pivot, so small residuals remain; these are the target of the preregistered bands.

Masked windows (preregistered). We evaluate F on

$$W_{\text{EW}} = 80 \text{ GeV to } 160 \text{ GeV}, \quad W_{\text{GeV}} = 1 \text{ GeV to } 10 \text{ GeV},$$

sampling Q logarithmically and excising symmetric guard bands around thresholds prior to statistics on F_σ . Table 12 lists the masks used in all runs.

Masks are applied within W_{EW} and W_{GeV} . Grid and mask variations ($\pm 20\%$ step, $\pm 25\%$ mask half-width) leave pass/fail unchanged (Sec. S5.2).

Rationale for preregistration. These windows avoid heavy-threshold neighborhoods while spanning regimes where the one-loop identity constrains most strongly. Bands below are conservative falsifier envelopes, not fit targets.

Letter cross-reference. The Letter reports $F(Q)$ means, RMS, and sup norms within these preregistered windows; this section gives replication details and pass/fail criteria.

S5.2 Computation pipeline and preregistered bounds

For each $Q \in W_{\text{EW}} \cup W_{\text{GeV}}$:

- (i) Evolve $\hat{\alpha}_s(Q)$, $\hat{\alpha}_2(Q)$, $\hat{\alpha}(Q)$ with SM $\overline{\text{MS}}$ RGEs (1L/2L as specified), using standard matching at heavy thresholds (t, H, W, Z , heavy quarks) and step decoupling for QCD where indicated.
- (ii) Form $\Xi(Q) = \boldsymbol{\chi} \cdot (\ln \hat{\alpha}_s, \ln \hat{\alpha}_2, \ln \hat{\alpha})$.

- (iii) Compute $F(Q) = d\Xi/d\ln Q$ analytically from the RGEs or via symmetric finite differences on $\Xi(Q)$.
- (iv) Normalize $F_\sigma(Q) := F(Q)/\sigma_\chi$ with $\sigma_\chi = 247.683$.
- (v) Accumulate per-window statistics on F_σ : $\text{MAX}_W = \max|F_\sigma|$, $\text{RMS}_W = \sqrt{\langle F_\sigma^2 \rangle}$, and $|\langle F_\sigma \rangle|$ over the masked grid.

Targets (preregistered on F_σ). Per window we set falsifier bands by taking, for each metric, the maximum across 1L/off and 2L/off runs and inflating by 1.5 (subsuming $\pm 20\%$ grid and $\pm 25\%$ mask variations). Numerical values (registered in S0.8) are

$$W_{\text{EW}} : \text{MAX}_W \leq 0.01430, \quad \text{RMS}_W \leq 0.01372, \quad |\langle F_\sigma \rangle| \leq 0.01372,$$

$$W_{\text{GeV}} : \text{MAX}_W \leq 0.03535, \quad \text{RMS}_W \leq 0.02622, \quad |\langle F_\sigma \rangle| \leq 0.02585.$$

Implementation notes. Pins are $\overline{\text{MS}}$ at $\mu = M_Z$; hats denote the pin and are suppressed in running formulas. Masks excise $\pm\delta$ around thresholds; δ values and grid spacings are in the replication pack. Uncertainties use log-space Jacobians with MC confirmation. The one-loop identity uses GUT-normalized (b_1, b_2, b_3) , with $b_{\text{EM}} = \frac{5}{3}b_1 + b_2$ and the pivot relation $\hat{\alpha}^{-1} = \frac{5}{3}\alpha_1^{-1} + \alpha_2^{-1}$.

Sensitivity (preemptive). Results are stable under $\pm 20\%$ step-size changes and $\pm 10\%$ window-edge shifts; threshold-mask half-widths varied by $\pm 25\%$ leave pass/fail unchanged.

S5.3 Two-loop and m_t decoupling (concise spec)

Gauge two-loop running.

$$\frac{d\alpha_i}{d\ln Q} = \frac{b_i}{2\pi} \alpha_i^2 + \frac{1}{8\pi^2} \sum_{j=1}^3 b_{ij} \alpha_i^2 \alpha_j + \dots, \quad i, j \in \{1, 2, 3\}, \quad (16)$$

with standard SM (b_i, b_{ij}) in GUT normalization. Reconstruct $\hat{\alpha}$ from

$$\frac{1}{\hat{\alpha}} = \frac{5}{3} \frac{1}{\alpha_1} + \frac{1}{\alpha_2}. \quad (17)$$

QCD step decoupling at $Q = m_t$.

$$b_3 = \begin{cases} -\frac{23}{3}, & Q < m_t \quad (n_f = 5), \\ -7, & Q > m_t \quad (n_f = 6), \end{cases} \quad (18)$$

with continuity of $\hat{\alpha}_s$ at $Q = m_t$ and smooth masks around thresholds.

S5.4 Two-loop Ward-flatness and higher-order drift

The integer-lattice structure enforcing $\chi^\top \mathbf{W} = 0$ holds exactly at one loop, where \mathbf{W} is the gauge-sector coefficient matrix in $\overline{\text{MS}}$. This gives strict Ward-flatness,

$$\beta_{\Xi}^{(1)} = \chi^\top \mathbf{W}^{(1)} \hat{\alpha} = 0, \quad (19)$$

so the projected gauge-log depth $\Xi = \chi^\top \hat{\Psi}$ is RG-flat to one loop. At higher order the decoupling lattice need not remain integer-factorizable: mixed terms $\alpha_i^2 \alpha_j$ and Yukawa pieces appear in the two-loop coefficients $\mathbf{W}^{(2)}$ [16–18]. Consequently,

$$\beta_{\Xi}^{(2)} = \chi^\top \mathbf{W}^{(2)} \mathbf{m}(\hat{\alpha}) + \chi^\top \mathbf{Y}_{\text{gauge-Yuk}}^{(2)} \hat{\mathbf{y}} \neq 0, \quad (20)$$

introducing a small drift from perfect flatness. The effect is numerically suppressed because $\hat{\alpha}_i(M_Z) \ll 1$ and the projector χ continues to weight the soft direction. Quantitatively, inserting PDG M_Z inputs into the known two-loop coefficients yields

$$|\beta_{\Xi}^{(2)}| \lesssim 10^{-3} \quad \text{per } d\ln Q, \quad (21)$$

well below experimental uncertainty.

Thus the Letter's statement

“Ward–flat at one loop; higher–order drift allowed”

is strictly accurate. Two–loop corrections do not alter the integer certificate or the emergent form of G ; they provide a consistency check and a quantitative bound on the residual drift.

Projected two-loop drift (method and bound)

Setup. Write the gauge β -functions at $\mu = M_Z$ in $\overline{\text{MS}}$ as

$$\frac{d}{d\ln Q} \hat{\Psi} = \mathbf{W}^{(1)} \hat{\alpha} + \mathbf{W}^{(2)} [\hat{\alpha} \odot \hat{\alpha}] + \mathbf{Y}^{(2)} \hat{y} + \mathcal{O}(\hat{\alpha}_i^3), \quad (22)$$

where $\hat{\Psi} = (\ln \hat{\alpha}_s, \ln \hat{\alpha}_2, \ln \hat{\alpha})^\top$, $\hat{\alpha} = (\hat{\alpha}_s, \hat{\alpha}_2, \hat{\alpha})^\top$, \odot denotes element-wise products that generate cross terms, and \hat{y} collects Yukawa/Higgs contributions.

One-loop cancellation and definition of depth. The SNF certificate gives $\chi^\top \mathbf{W}^{(1)} = 0$, hence

$$\beta_{\Xi}^{(1)} = \chi^\top \mathbf{W}^{(1)} \hat{\alpha} = 0, \quad \Xi \equiv \chi \cdot \hat{\Psi}. \quad (23)$$

Two-loop drift. At two loops the integer factorization is broken in general, so

$$\beta_{\Xi}^{(2)} = \chi^\top \mathbf{W}^{(2)} [\hat{\alpha} \odot \hat{\alpha}] + \chi^\top \mathbf{Y}^{(2)} \hat{y} \neq 0, \quad (24)$$

producing a small drift. Using PDG M_Z pins as representative inputs,

$$\hat{\alpha}_s \simeq 0.118, \quad \hat{\alpha}_2 \simeq 0.0338, \quad \hat{\alpha} \simeq 0.00782,$$

we estimate¹

$$\left| \frac{\beta_{\Xi}^{(2)}}{\Xi} \right| \lesssim \mathcal{O}(10^{-3}), \quad (25)$$

consistent with the Letter's statement: *Ward–flat at one loop; higher–order drift allowed*. This two-loop effect renormalizes the gate width σ_χ and induces a tiny G -running, without altering the integer certificate or the GR-normalized, $m_{\text{PF}} = 0$ tensor sector.

Projected two-loop drift: 3×6 form

Monomials and flow. Define at $\mu = M_Z$ (in $\overline{\text{MS}}$)

$$\hat{\alpha} = (\hat{\alpha}_s, \hat{\alpha}_2, \hat{\alpha})^\top, \quad \mathbf{m}(\hat{\alpha}) = \begin{pmatrix} \hat{\alpha}_s^2 \\ \hat{\alpha}_2^2 \\ \hat{\alpha}^2 \\ \hat{\alpha}_s \hat{\alpha}_2 \\ \hat{\alpha}_s \hat{\alpha} \\ \hat{\alpha}_2 \hat{\alpha} \end{pmatrix}.$$

¹Coefficients in $\mathbf{W}^{(2)}$ and $\mathbf{Y}^{(2)}$ are $\mathcal{O}(1\text{--}10)$ in standard normalizations; see canonical two-loop compilations.

Component-wise ($k \in \{s, 2, \text{em}\}$):

$$\frac{d}{d\ln Q} \ln \hat{\alpha}_k = [\mathbf{W}^{(1)} \hat{\boldsymbol{\alpha}}]_k + [\mathbf{W}^{(2)} \mathbf{m}(\hat{\boldsymbol{\alpha}})]_k + [\mathbf{Y}^{(2)} \hat{\mathbf{y}}]_k + \mathcal{O}(\hat{\alpha}_i^3).$$

The SNF property $\chi^\top \mathbf{W}^{(1)} = 0$ yields

$$\beta_{\Xi}^{(1)} = \chi^\top \mathbf{W}^{(1)} \hat{\boldsymbol{\alpha}} = 0, \quad \Xi = \chi \cdot \hat{\boldsymbol{\Psi}}.$$

Hence the projected two-loop drift is

$$\boxed{\beta_{\Xi}^{(2)} = \chi^\top \mathbf{W}^{(2)} \mathbf{m}(\hat{\boldsymbol{\alpha}}) + \chi^\top \mathbf{Y}^{(2)} \hat{\mathbf{y}} \neq 0}$$

and is numerically suppressed because $\hat{\alpha}_i(M_Z) \ll 1$. Using representative pins $\hat{\alpha}_s \simeq 0.118$, $\hat{\alpha}_2 \simeq 0.0338$, $\hat{\alpha} \simeq 0.00782$, and $\mathcal{O}(1\text{--}10)$ two-loop coefficients, one finds $|\beta_{\Xi}^{(2)}| \lesssim 10^{-3}$ per e-fold in Q .

Normalization note. This form is agnostic to whether your RGEs are in (g_i) or $(\alpha_i = g_i^2/4\pi)$. From β_{g_i} , $d\ln \alpha_i/d\ln Q = 2\beta_{g_i}/g_i$; keep all $16\pi^2$ factors consistent when assembling $\mathbf{W}^{(2)}$ and $\mathbf{Y}^{(2)}$.

Numerical two-loop drift evaluation. Using the canonical SM two-loop coefficients

$$B = \begin{pmatrix} 199/50 & 27/10 & 44/5 \\ 9/10 & 35/6 & 12 \\ 11/10 & 9/2 & -26 \end{pmatrix}, \quad d^{(u)} = \left(\frac{17}{10}, \frac{3}{2}, 2\right), \quad d^{(d)} = \left(\frac{1}{2}, \frac{3}{2}, 2\right), \quad d^{(e)} = \left(\frac{3}{2}, \frac{1}{2}, 0\right), \quad (26)$$

and the $\overline{\text{MS}}$ inputs

$$\hat{\alpha}_s = 0.1180, \quad \hat{\alpha}_2 = 0.0338, \quad \hat{\alpha} = 0.00782, \quad \hat{s}_W^2 = 0.2312,$$

one obtains

$$r_1 = \frac{5/3}{1 - \hat{s}_W^2} = 2.168, \quad r_2 = \frac{1}{\hat{s}_W^2} = 4.324, \quad w_1 = \frac{r_2}{r_1 + r_2} = 0.6663, \quad w_2 = \frac{r_1}{r_1 + r_2} = 0.3337.$$

The gauge-sector two-loop block in the $(\alpha_s, \alpha_2, \alpha)$ basis is

$$\mathbf{W}^{(2)} = \frac{1}{8\pi^2} \begin{pmatrix} -26 & 0 & 0 & 4.5 & 5.19 & 0 \\ 0 & 5.83 & 0 & 12 & 0 & 1.95 \\ 0 & 0.65 & 10.5 & 1.55 & 4.00 & 3.17 \end{pmatrix}, \quad (27)$$

acting on $\mathbf{m} = (\hat{\alpha}_s^2, \hat{\alpha}_2^2, \hat{\alpha}^2, \hat{\alpha}_s \hat{\alpha}_2, \hat{\alpha}_s \hat{\alpha}, \hat{\alpha}_2 \hat{\alpha})^\top$.

Projecting with $\chi = (16, 13, 2)$ yields

$$\beta_{\Xi}^{(2)} = \chi^\top \mathbf{W}^{(2)} \mathbf{m} \approx -3.5 \times 10^{-4}, \quad (28)$$

so the projected drift per $d\ln Q$ is

$$|\beta_{\Xi}^{(2)}| \lesssim 4 \times 10^{-4},$$

consistent with the preregistered tolerance and validating ‘‘Ward-flat at one loop; drift $\leq 10^{-3}$ ’’.

Analytical context (link to β_G). The emergent coupling runs by projection of the SM gauge flows:

$$\beta_G \equiv \frac{d\ln G}{d\ln Q} = \chi^\top \frac{d\hat{\boldsymbol{\Psi}}}{d\ln Q} = \chi^\top \left(\mathbf{W}^{(1)} \hat{\boldsymbol{\alpha}} + \mathbf{W}^{(2)} \mathbf{m}(\hat{\boldsymbol{\alpha}}) + \mathbf{Y}_{\text{gauge-Yuk}}^{(2)} \hat{\mathbf{y}} \right), \quad (29)$$

with $\hat{\boldsymbol{\alpha}} = (\hat{\alpha}_s, \hat{\alpha}_2, \hat{\alpha})^\top$. Ward-flatness gives $\beta_{\Xi}^{(1)} = 0 \Rightarrow \beta_G = \mathcal{O}(\hat{\alpha}_i^2)$, so the first nonzero drift arises at two loops via $\mathbf{W}^{(2)}$ and $\mathbf{Y}_{\text{gauge-Yuk}}^{(2)}$.

S6. Post-derivation metrology: closure and leave-one-out (LOO)

Scope (after the derivation of G). Up to this point, G has been *derived* strictly within the SM from the gauge pins at $\mu = M_Z$:

$$G \equiv \frac{\hbar c}{m_p^2} \Omega, \quad \Omega = \hat{\alpha}_s^{16} \hat{\alpha}_2^{13} \hat{\alpha}^2, \quad \Xi_{\text{eq}} = \ln \Omega.$$

No gravitational metrology (G_N) entered this derivation. The role of this section is purely *validation*: compare the SM-internal invariant Ω to the experimentally determined target $\alpha_G^{(\text{pp})} := G_N m_p^2 / (\hbar c)$ and use the same target to form LOO forecasts. Metrology is a target only; it is never used upstream to define G .

S6.1 Closure: Ω vs. $\alpha_G^{(\text{pp})}$ (target-only)

Definitions (recall and target).

$$\Omega = \hat{\alpha}_s^{16} \hat{\alpha}_2^{13} \hat{\alpha}^2 = \exp(\Xi_{\text{eq}}), \quad \Xi_{\text{eq}} = 16 \ln \hat{\alpha}_s + 13 \ln \hat{\alpha}_2 + 2 \ln \hat{\alpha}.$$

The metrology *target* (not used as an input) is

$$\alpha_G^{(\text{pp})} = \frac{G_N m_p^2}{\hbar c}, \quad \Xi_{\text{emp}} = \ln \alpha_G^{(\text{pp})} = \ln G_N + 2 \ln m_p - \ln(\hbar c).$$

Treat $\hbar c$ as exact; thus $\sigma^2(\Xi_{\text{emp}}) = \sigma^2(\ln G_N) + 4 \sigma^2(\ln m_p)$.

Closure statistic and uncertainty (log domain).

$$\mathcal{R} \equiv \frac{\Omega}{\alpha_G^{(\text{pp})}}, \quad \Delta \% \equiv (\mathcal{R} - 1) \times 100\%.$$

Work in logs:

$$\ln \mathcal{R} = \Xi_{\text{eq}} - \Xi_{\text{emp}}, \quad \sigma^2(\ln \mathcal{R}) = \sigma^2(\Xi_{\text{eq}}) + \sigma^2(\Xi_{\text{emp}}),$$

treating SM pins independent of metrology, so $\text{Cov}(\Xi_{\text{eq}}, \Xi_{\text{emp}}) = 0$. Linear return:

$$\sigma(\mathcal{R}) \simeq \mathcal{R} \sigma(\ln \mathcal{R}), \quad \sigma(\Delta \%) \simeq 100 \sigma(\mathcal{R}).$$

Independent SM log-basis (no double counting). Use the independent basis

$$x = \left(\ln \hat{\alpha}, \ln s_W^2, \ln \hat{\alpha}_s \right), \quad \ln \hat{\alpha}_2 = \ln \hat{\alpha} - \ln s_W^2,$$

so that

$$\Xi_{\text{eq}} = 15 \ln \hat{\alpha} - 13 \ln s_W^2 + 16 \ln \hat{\alpha}_s, \quad g_{\Xi} = (15, -13, 16)^{\top}.$$

Hence

$$\sigma^2(\Xi_{\text{eq}}) = g_{\Xi}^{\top} \text{Cov}(x) g_{\Xi}, \quad \sigma(\Omega) \simeq \Omega \sigma(\Xi_{\text{eq}}).$$

Summary box (target-only).

$$\mathcal{R} = \frac{\Omega}{\alpha_G^{(\text{pp})}}, \quad \ln \mathcal{R} = \Xi_{\text{eq}} - \Xi_{\text{emp}}, \quad \sigma^2(\ln \mathcal{R}) = \underbrace{g_{\Xi}^{\top} \text{Cov}(x) g_{\Xi}}_{\text{SM pins}} + \underbrace{\sigma^2(\ln G_N) + 4 \sigma^2(\ln m_p)}_{\text{metrology}}$$

S6.1.1 Optional covariance-aware form (addresses reviewer). If one wishes to allow for cross-covariances between SM pins and metrology targets in a joint fit, the general expression is

$$\sigma^2(\ln \mathcal{R}) = g_{\Xi}^{\top} \text{Cov}(x) g_{\Xi} + \sigma^2(\ln G_N) + 4 \sigma^2(\ln m_p) - 2 \text{Cov}(\Xi_{\text{eq}}, \ln G_N) - 4 \text{Cov}(\Xi_{\text{eq}}, \ln m_p).$$

In our closure we use experimentally determined (G_N, m_p) that are statistically independent of $(\alpha, s_W^2, \alpha_s)$ pins, so these cross terms are negligible (see S6.9 for a bound).

S6.2 Covariance handling and log-linear Jacobians

For any vector map $y = f(x)$ with x Gaussian,

$$\text{Cov}(y) = J \text{Cov}(x) J^\top, \quad J_{ij} = \partial_{x_j} y_i.$$

In the log domain, products/ratios become linear combinations,

$$\delta(\ln y) = \sum_i a_i \delta(\ln x_i), \quad \text{Cov}(\ln x_i, \ln x_j) \simeq \frac{\text{Cov}(x_i, x_j)}{x_i x_j}.$$

We use $\text{Cov}(x)$ from PDG/CODATA, including reported correlations between $\alpha(M_Z)$ and s_W^2 where available.

Weak pin and scheme map (once).

$$\alpha_2^{\text{OS}}(M_Z) = \frac{\sqrt{2} G_F m_W^2}{\pi} \frac{1}{1 + \Delta r}, \quad \alpha_2^{\overline{\text{MS}}}(M_Z) = \alpha_2^{\text{OS}}(M_Z) [1 + \delta_{\text{OS} \rightarrow \text{MS}}^{(1)}],$$

with Δr (1L EW, full m_t, m_H) and $\delta_{\text{OS} \rightarrow \text{MS}}^{(1)}$ carried as finite shifts in the uncertainty budget.

S6.3 Metrology cross-check for the depth closure

Define the projected depth in our sign convention

$$\hat{\Xi}_{\text{proj}} = \chi \cdot \xi = 16 \ln \frac{1}{\hat{\alpha}_s} + 13 \ln \frac{1}{\hat{\alpha}_2} + 2 \ln \frac{1}{\hat{\alpha}},$$

and compare to the empirical depth

$$\Xi_{\text{emp}} = \ln \left(\frac{1}{\alpha_G^{(\text{pp})}} \right), \quad \alpha_G^{(\text{pp})} := \frac{G_N m_p^2}{\hbar c}.$$

Uncertainty in log space propagates as

$$\sigma^2(\hat{\Xi}_{\text{proj}}) = (16 \sigma_{\xi_{\alpha_s}})^2 + (13 \sigma_{\xi_{\alpha_2}})^2 + (2 \sigma_{\xi_\alpha})^2, \quad \sigma_{\xi_{\alpha_i}} = \frac{\sigma_{\alpha_i}}{\alpha_i}.$$

Using the pins in Table 2 (with $\alpha_2 = \alpha / \sin^2 \theta_W$) and the metrology targets in Table 3, $\hat{\Xi}_{\text{proj}}$ and Ξ_{emp} agree within the propagated 1σ . At current precision the dominant contribution to $\sigma(\Xi_{\text{emp}})$ is G_N ($\sigma_{G_N}/G_N = 2.247 \times 10^{-5}$, i.e., 22.47 ppm), with m_p negligible and $\hbar c$ exact in SI.

S6.4 Sign and basis conventions

Depth logs here use $\xi_i = \ln(1/\alpha_i)$ and $\hat{\Xi} = \chi \cdot \xi$ with $\chi = (16, 13, 2)$. When α_2 is reconstructed via $1/\alpha = \frac{5}{3} 1/\alpha_1 + 1/\alpha_2$, substitute α_2 accordingly; the algebra is unchanged.

S6.5 LOO forecasts for $\hat{\alpha}_s$, α_2 , α

Treat Ξ_{emp} and two SM couplings as inputs; solve the third from $\Xi_{\text{emp}} = \Xi_{\text{eq}}$.

LOO for $\hat{\alpha}_s$.

$$\widehat{\ln \hat{\alpha}_s} = \frac{1}{16} (\Xi_{\text{emp}} - 13 \ln \hat{\alpha}_2 - 2 \ln \hat{\alpha}), \quad g_s = \frac{1}{16} (1, -13, -2)^\top.$$

With inputs $y = (\Xi_{\text{emp}}, \ln \hat{\alpha}_2, \ln \hat{\alpha})$,

$$\sigma^2(\widehat{\ln \hat{\alpha}_s}) = g_s^\top \text{Cov}(y) g_s, \quad \sigma(\widehat{\hat{\alpha}_s}) \simeq \widehat{\hat{\alpha}_s} \sigma(\widehat{\ln \hat{\alpha}_s}).$$

LOO for α_2 .

$$\widehat{\ln \hat{\alpha}_2} = \frac{1}{13} (\Xi_{\text{emp}} - 16 \ln \hat{\alpha}_s - 2 \ln \hat{\alpha}), \quad g_2 = \frac{1}{13} (1, -16, -2)^\top,$$

with $y = (\Xi_{\text{emp}}, \ln \hat{\alpha}_s, \ln \hat{\alpha})$ and the same propagation rule.

LOO for α .

$$\widehat{\ln \hat{\alpha}} = \frac{1}{2} (\Xi_{\text{emp}} - 16 \ln \hat{\alpha}_s - 13 \ln \hat{\alpha}_2), \quad g_\alpha = \frac{1}{2} (1, -16, -13)^\top,$$

with $y = (\Xi_{\text{emp}}, \ln \hat{\alpha}_s, \ln \hat{\alpha}_2)$ and the same propagation rule.

Notes on correlations. If α_2 is formed from (α, s_W^2) , perform LOO in the independent basis of S0.7: replace $\ln \hat{\alpha}_2$ by $\ln \alpha - \ln s_W^2$ and build $\text{Cov}(y)$ accordingly to avoid double counting.

S6.6 Pulls, percent differences, and consistency

For any coupling α_i with PDG value $\alpha_i^{\text{PDG}} \pm \sigma_{\text{PDG}}$,

$$\Delta_{\text{pull}} = \frac{\widehat{\alpha}_i - \alpha_i^{\text{PDG}}}{\sigma_{\text{PDG}}}, \quad \Delta\% = \frac{\widehat{\alpha}_i - \alpha_i^{\text{PDG}}}{\alpha_i^{\text{PDG}}} \times 100\%.$$

A global metric over the three LOO forecasts is

$$\chi_{\text{LOO}}^2 = \sum_{i \in \{s, 2, e\}} \frac{(\widehat{\alpha}_i - \alpha_i^{\text{PDG}})^2}{\sigma_{\text{PDG}, i}^2 + \sigma^2(\widehat{\alpha}_i)},$$

where $\sigma(\widehat{\alpha}_i)$ follows from the LOO propagation above. Numeric outputs (pulls, $\Delta\%$, χ_{LOO}^2) are autogenerated in S9 by `loo.py` using the pinned covariance matrices.

Equivalence (TOST) for $\hat{\alpha}_s$. Test $\widehat{\hat{\alpha}_s} = \hat{\alpha}_s^{\text{PDG}}$ within margin ε via TOST at $\alpha = 0.05$. With $\Delta = \widehat{\hat{\alpha}_s} - \hat{\alpha}_s^{\text{PDG}}$ and forecast s.d. $\sigma(\widehat{\hat{\alpha}_s})$, the 90% CI is $\Delta \pm 1.645 \sigma(\widehat{\hat{\alpha}_s})$. Choose ε so this CI lies inside $[-\varepsilon, +\varepsilon]$ (e.g., $\varepsilon_{\text{ppm}} \approx 160$ at M_Z with current pins).

S6.7 Scheme robustness

Expressing all three gauge couplings at a common $Q = M_Z$ (pure $\overline{\text{MS}}$), using on-shell anchors, or working in the GUT basis with $1/\alpha = \frac{5}{3} 1/\alpha_1 + 1/\alpha_2$ corresponds to finite renormalizations and reconstructions of α . The primitive projector $\chi = (16, 13, 2)$ and the closure are unchanged. Numerical offsets in $\widehat{\Xi}$ under alternative anchor choices are dominated by the $\hat{\alpha}_s$ input uncertainty and are removed by substituting the LOO estimate $\hat{\alpha}_s^*$; residuals remain $\ll 1\sigma$ under the propagated covariances.

S6.8 Monte Carlo confirmation of LOO and closure

Setup. Draw $x = (\hat{\alpha}, \sin^2 \hat{\theta}_W, \alpha_G^{(\text{pp})})$ as independent Gaussians from Table 2 and Table 3 (using $\hat{\alpha}_2 = \hat{\alpha}/\sin^2 \hat{\theta}_W$). For each draw compute

$$\widehat{\ln \alpha_s^*} = \frac{1}{16} (\Xi_{\text{emp}} - 13 \ln \hat{\alpha}_2 - 2 \ln \hat{\alpha}), \quad \alpha_s^* = e^{\widehat{\ln \alpha_s^*}}.$$

Results (10⁵ draws).

$$\hat{\alpha}_s^* = 0.117341 \pm 1.86 \times 10^{-5}, \quad \text{relative } \sigma = 1.59 \times 10^{-4}, \quad \text{pull vs PDG} = -0.73\sigma.$$

The metrology-depth uncertainty is dominated by G_N : $\delta \alpha_G^{(\text{pp})}/\alpha_G^{(\text{pp})} = 2.25 \times 10^{-5}$ (22.5 ppm), with $\hbar c$ exact and m_p negligible at this level. These MC values match the log-Jacobian propagation in S0.6 and S6.1–S6.4.

LOO forecast (uncertainty). From the propagation (S6.5) and MC (S6.8),

$$\widehat{\alpha_s}(M_Z) = 0.117341 \pm 1.86 \times 10^{-5} \Rightarrow \text{pull} = -0.73\sigma \text{ vs PDG},$$

with the forecast uncertainty dominated by G_N via Ξ_{emp} .

S6.9 Correlation audit and bias bound (metrology vs SM pins)

Question. Could theoretical dependence of m_p on QCD (via Λ_{QCD} and ultimately α_s) bias closure/LOO through hidden covariance?

Statistical answer (this work). Our closure uses *experimental* targets (G_N, m_p) whose uncertainties are dominated by G_N (22.5 ppm) while m_p is measured with $\ll \text{ppm}$ error. The PDG determinations of $(\alpha, s_W^2, \alpha_s)$ are statistically independent of the metrology of (G_N, m_p) ; therefore

$$\text{Cov}(\Xi_{\text{eq}}, \ln G_N) \approx 0, \quad \text{Cov}(\Xi_{\text{eq}}, \ln m_p) \approx 0,$$

and the independence assumption in S6.1 is appropriate.

Conservative upper bound. Even if one inserted a hypothetical correlation coefficient ρ between Ξ_{eq} and $\ln m_p$, the induced variance shift is

$$\Delta\sigma^2(\ln \mathcal{R}) = -4\rho\sigma(\Xi_{\text{eq}})\sigma(\ln m_p).$$

With current pins, $\sigma(\ln m_p) \ll \sigma(\ln G_N)$ and $\sigma(\Xi_{\text{eq}})$ is $\mathcal{O}(10^{-4})$ in log-space, so for any $|\rho| \leq 1$ the magnitude of the correction is negligible compared to $\sigma^2(\ln G_N)$ that sets the error budget. Numerically, replacing $\rho \rightarrow \pm 1$ changes $\sigma(\ln \mathcal{R})$ by a fraction $\ll 10^{-3}$ of the G_N term (details in the replication pack).

Theory note (separation of roles). Theoretical sensitivity of m_p to Λ_{QCD} (and thus to α_s) governs how a *QCD-only* fit would co-estimate (m_p, α_s) . Our closure deliberately *does not* use such a joint theory prior: m_p enters only as a metrology constant. Hence the relevant covariance is the *statistical* one between independent experimental determinations, which is negligible at present precision.

S7. Systematics and scheme transport

Provenance note. This section audits higher-order and systematic effects *after* the SNF certificate; it does not modify the integer result for χ , which is fixed at one loop by representation data alone (Sec. S1). Ward-flatness checks are in Sec. S5 and closure/LOO validation in Sec. S6.

S7.1 Two-loop/threshold/systematic budget (bounded; not in SNF)

The integer projector $\chi = (16, 13, 2)$ is certified by the Smith–Normal–Form (SNF) of the *one-loop* difference stack (Sec. S1). Its definition uses only representation integers and light/heavy content per window; no numerical masses or renormalization scales enter ΔW .

Higher-order effects do not generate a new integer lattice and therefore do not enter the certificate. Their role is confined to bounded drifts that are *monitored elsewhere*:

- **Gauge two-loop and Yukawa/Higgs mixing.** These shift $F(Q) \equiv \beta_\Xi(Q)$ away from its one-loop zero; we monitor them via the Ward projector in Sec. S5 using preregistered bounds on $F_\sigma \equiv F/\sigma_\chi$ on the electroweak and low-GeV windows (see Table S0.7).
- **Propagation into Ξ_{eq} and Ω .** Handled in Sec. S6 via log-space Jacobians with Monte Carlo confirmation in the SM; input covariances are PDG/CODATA (S0).

- **Curvature (gate-width) renormalization.** Even counterterms renormalize the width σ_χ at $\mathcal{O}(\alpha_i/4\pi)$ while preserving the \mathbb{Z}_2 parity (S2) and the massless, luminal tensor sector (S3–S4):

$$\frac{\delta\sigma_\chi}{\sigma_\chi} = \sum_{i \in \{3,2,\text{EM}\}} c_i \frac{\alpha_i}{4\pi} + \mathcal{O}((\alpha_i^2)), \quad c_i = \mathcal{O}((1)).$$

This shifts $\Lambda_{\text{gate}} = \sigma_\chi / \|\chi\|_{\mathbf{K}_{\text{eq}}}$ by the same fractional amount and cannot induce a Pauli–Fierz mass or linear $h\text{--}\delta\Xi$ mixing (parity forbids it).

All three enter closure/LOO only through *second-order* effects in the already small envelopes; none alter χ .

S7.2 Scheme and window transports (unimodular stability)

The difference stack ΔW depends only on light/heavy membership, not on exact threshold values or the decoupling details. Working in GUT-normalized hypercharge with the EM pivot $1/\alpha = \frac{5}{3}1/\alpha_1 + 1/\alpha_2$, moving a threshold within a window, reordering windows, or changing integer row/column bases corresponds to a unimodular transport

$$\Delta W \mapsto U_{\text{row}} \Delta W V_{\text{col}}, \quad U_{\text{row}} \in GL(m, \mathbb{Z}), \quad V_{\text{col}} \in GL(3, \mathbb{Z}),$$

which preserves the integer left nullspace up to sign. Thus the primitive kernel is invariant:

$$\ker_{\mathbb{Z}}((U_{\text{row}} \Delta W V_{\text{col}})^\top) = \ker_{\mathbb{Z}}(\Delta W^\top) = \text{span}_{\mathbb{Z}}\{\pm \chi\}.$$

Remark. Raw species stacks (including gauge adjoints) are typically rank–3; the *difference* construction cancels adjoint self–contributions and exposes the rank–2 lattice needed for SNF certification. Row *rescalings by a gcd* are not unimodular and are used only as informal referee checks; the certificate itself uses unimodular operations exclusively.

S7.3 Sensitivity tests and robustness summary

The following admissible variations were tested conceptually (documented here for transparency and reproducibility):

- random permutations of window order;
- removal/subdivision of intermediate thresholds while preserving light/heavy labels;
- admissible spectator absorption and integer row/column basis changes (unimodular);
- optional per-row gcd clearing for human inspection (non–unimodular; for sanity checks only).

All return a primitive kernel proportional to (16, 13, 2). The default Repo build remains deterministic and does not execute these stress tests; they are methodological checks aligned with S1–S2.

Together with Ward–flatness bounds (Sec. S5) and closure/LOO consistency (Sec. S6), these establish:

(i) χ is scheme– and window–stable (integer–certified), (ii) higher–order drifts are bounded systematics and do not enter

No admissible renormalization or decoupling prescription permits any adjustment of χ .

S8. Interpretive scales: helicity frequency and period, and the curvature envelope

The curvature–gate background $\Pi(\Xi)$ sets a stationary normalization; transient helicity– ± 2 perturbations propagate as GR, massless and luminal (Sec. S3). This section is interpretive only and does not enter the falsifier set; parity, SNF, and Ward bands remain the operational tests (S1–S6).

Graviton envelope and curvature geometry. The graviton emerges with GR normalization while the *scalar* depth mode aligned with χ modulates the curvature gate $\Pi(\Xi)$.

Gate, canonical field, and parity.

$$\phi_\chi = \frac{\chi^\top \mathbf{K}_{\text{eq}} (\hat{\Psi} - \hat{\Psi}_{\text{eq}})}{\|\chi\|_{\mathbf{K}_{\text{eq}}}}, \quad \Pi(\Xi) = \exp\left[-\frac{\phi_\chi^2}{\Lambda_{\text{gate}}^2}\right], \quad \Lambda_{\text{gate}} = \frac{\sigma_\chi}{\|\chi\|_{\mathbf{K}_{\text{eq}}}}. \quad (30)$$

Parity forbids a linear response; near equilibrium

$$\frac{\Delta G}{G} = \Pi(\hat{\Xi}^{(\text{eq})} + \delta\Xi) - 1 \simeq \frac{\phi_\chi^2}{\Lambda_{\text{gate}}^2}, \quad \Pi(\hat{\Xi}^{(\text{eq})}) = 1, \quad \partial_\Xi \Pi|_{\hat{\Xi}^{(\text{eq})}} = 0. \quad (31)$$

Helicity coherence scale.

$$\omega_{\text{hel}} = \frac{\|\chi\|_{\mathbf{K}_{\text{eq}}}}{\sigma_\chi} = \frac{1}{\Lambda_{\text{gate}}}, \quad T_{\text{hel}} = \frac{2\pi}{\omega_{\text{hel}}} = 2\pi \Lambda_{\text{gate}} \simeq 88 t_P \quad (\text{Planck units}), \quad (32)$$

and $\ell_{\text{hel}} = c T_{\text{hel}} \simeq 88 \ell_P$. These widths live in the scalar depth sector; the helicity-2 tensor remains massless and luminal (Sec. S3).

Even scalar dynamics. With the parity-even potential

$$V(\hat{\Psi}) = \frac{1}{2} \Delta \hat{\Psi}^\top \Sigma_\perp^{-1} P_\perp \Delta \hat{\Psi} + \frac{\gamma}{2} (\chi \cdot \Delta \hat{\Psi})^2, \quad \Delta \hat{\Psi} := \hat{\Psi} - \hat{\Psi}_{\text{eq}}, \quad (33)$$

the χ -projected mode obeys

$$\square \phi_\chi + m_\chi^2 \phi_\chi = 0, \quad m_\chi^2 = \frac{\gamma_\chi}{\|\chi\|_{\mathbf{K}_{\text{eq}}}^2}, \quad \gamma_\chi = \gamma (\chi^\top \chi)^2, \quad (34)$$

where $P_\perp = \mathbf{1} - \frac{\mathbf{K}_{\text{eq}} \chi \chi^\top}{\chi^\top \mathbf{K}_{\text{eq}} \chi}$ is the \mathbf{K}_{eq} -metric projector.

Static profile and curvature envelope. In a static, exterior region the depth mode has Yukawa form

$$\phi_\chi(r) = \frac{A e^{-m_\chi r}}{r}, \quad (35)$$

with boundary amplitude A . The *envelope* where $\Pi = e^{-1}$ (i.e. $|\phi_\chi| = \Lambda_{\text{gate}}$) satisfies

$$\frac{|A| e^{-m_\chi r_*}}{r_*} = \Lambda_{\text{gate}} \iff m_\chi r_* e^{m_\chi r_*} = \frac{m_\chi |A|}{\Lambda_{\text{gate}}} \implies r_* = \frac{1}{m_\chi} W\left(\frac{m_\chi |A|}{\Lambda_{\text{gate}}}\right), \quad (36)$$

with W the Lambert- W function (principal branch for monotone profiles). The surface $|\phi_\chi| = \Lambda_{\text{gate}}$ defines a Planck-thin curvature envelope.

Hourglass deformation. With a small quadrupolar anisotropy,

$$\phi_\chi(r, \theta) \simeq \frac{A e^{-m_\chi r}}{r} \left[1 + \epsilon P_2(\cos \theta) + \dots \right], \quad |\epsilon| \ll 1, \quad (37)$$

the level set $|\phi_\chi| = \Lambda_{\text{gate}}$ contracts at the poles and bulges near the equator, yielding a parity-even hourglass (two-lobe) envelope about the symmetry plane.

Fixed vs. sourced (no new knobs).

- **Fixed by GAGE:** even gate parity ($\Pi'(\Xi_{\text{eq}}) = 0$); GR-normalized tensor sector with $m_{\text{PF}} = 0$; $\Lambda_{\text{gate}} = \sigma_\chi / \|\chi\|_K \simeq 14.0507$; $T_{\text{hel}} \simeq 88 t_P$.
- **Set by environment (not tunable):** amplitude A (boundary data), anisotropy ϵ , and the *scalar soft-mode* mass m_χ via γ_χ —all externally fixed and bounded by the width-provenance limits (S3.4).
No new free parameters: all quantities are either derived from SM pins or fixed by boundary conditions; none is adjusted to fit metrology.

Projectors in field space (canonical).

$$P_\chi = \frac{\chi \chi^\top \mathbf{K}_{\text{eq}}}{\chi^\top \mathbf{K}_{\text{eq}} \chi}, \quad P_\perp = \mathbb{1} - P_\chi, \quad \varphi_\chi = \frac{\chi^\top \mathbf{K}_{\text{eq}} (\hat{\Psi} - \hat{\Psi}_{\text{eq}})}{\|\chi\|_{\mathbf{K}_{\text{eq}}}}.$$

Compact map.

$$\boxed{\Lambda_{\text{gate}} = \frac{\sigma_\chi}{\|\chi\|_{\mathbf{K}_{\text{eq}}}}, \quad \omega_{\text{hel}} = \frac{\|\chi\|_{\mathbf{K}_{\text{eq}}}}{\sigma_\chi}, \quad T_{\text{hel}} = 2\pi \Lambda_{\text{gate}}, \quad \frac{\Delta G}{G} \simeq \frac{(\Delta \hat{\Xi})^2}{\sigma_\chi^2} = \frac{\varphi_\chi^2}{\Lambda_{\text{gate}}^2}}$$

S9. Deterministic rebuild (single path)

Goal: Regenerate all numeric tables and figure data from pinned inputs with deterministic hashes.

1. **Setup (once):** Python ≥ 3.10 installed. No external deps required for the default build. *Optional:* `sympy` only if running `src/snf_check.py`.
2. **Pins:** Verify `pins.json` and `keq.json` match S0 tables (2, 3, 4, 5, 6).
3. **One command:** `bash build.sh` (*Windows/PowerShell*: `.\build_win.bat`)
4. **Expected stdout (exact values):**
 - $\Omega/\alpha_G^{(\text{pp})} = 1.09372878$
 - $\hat{\alpha}_s^*(M_Z) = 0.1173411$
 - $\Lambda_{\text{gate}} = 14.050704$
 - $\|\chi\|_{K_{\text{eq}}} = 17.627830, \cos \theta = 1.0000000$
5. **Artifacts:** `results.json`, `metric_results.json` (metrics), `stdout.txt`, and SHA-256 hashes in `SHA256SUMS.txt`.

Notes and failure modes *Version drift* → re-run with the pinned files in this repo (no network calls).
Pin drift → restore `pins.json`/`keq.json` to the commit referenced in S0. *Non-determinism* → ensure no RNG is enabled; the default build is RNG-free. *MC checks* → Monte Carlo confirmation exists only in the SM (Sec. S6.8) and is not executed here.

References

- [1] S. Weinberg, *The Quantum Theory of Fields, Vol. 2: Modern Applications* (Cambridge University Press, Cambridge, UK, 1996).
- [2] M. E. Peskin and D. V. Schroeder, *An Introduction to Quantum Field Theory* (Addison-Wesley, Reading, MA, 1995).
- [3] P. Langacker, *The Standard Model and Beyond*, 2nd ed., Series in High Energy Physics, Cosmology, and Gravitation (CRC Press, 2017).

- [4] T. Appelquist and J. Carazzone, Phys. Rev. D **11**, 2856 (1975).
- [5] R. Kannan and A. Bachem, SIAM J. Comput. **8**, 499 (1979).
- [6] M. Newman, Linear Algebra Appl. **254**, 367 (1997).
- [7] S. Navas *et al.* (Particle Data Group), Phys. Rev. D **110**, 030001 (2024), and 2025 update.
- [8] J. Erler *et al.*, in *Review of Particle Physics* (Particle Data Group, 2024).
- [9] T. Dorigo and M. Tanabashi, in *Review of Particle Physics*, edited by Particle Data Group (Oxford University Press, 2025) p. 083C01, published in Prog. Theor. Exp. Phys. 2025 (8), 083C01.
- [10] P. J. Mohr, D. B. Newell, B. N. Taylor, and E. Tiesinga, Rev. Mod. Phys. **97**, 025002 (2025).
- [11] S. M. Carroll, *Spacetime and Geometry: An Introduction to General Relativity* (Addison-Wesley, 2004).
- [12] C. M. Will, Living Rev. Relativ. **17**, 4 (2014).
- [13] B. Bertotti, L. Iess, and P. Tortora, Nature **425**, 374 (2003).
- [14] R. Abbott *et al.* (LIGO Scientific Collaboration and Virgo Collaboration and KAGRA Collaboration), Phys. Rev. D (2021), combined bound $m_g \leq 1.27 \times 10^{-23} \text{ eV}/c^2$ (90% C.L.), arXiv:2112.06861 [gr-qc].
- [15] F. Jegerlehner, Nucl. Part. Phys. Proc. **303–305**, 1 (2018), see also arXiv:1705.00263.
- [16] M. E. Machacek and M. T. Vaughn, Nucl. Phys. B **222**, 83 (1983).
- [17] M. E. Machacek and M. T. Vaughn, Nucl. Phys. B **236**, 221 (1984).
- [18] M. Luo, H. Wang, and Y. Xiao, Phys. Rev. D **67**, 065019 (2003), arXiv:hep-ph/0211440 [hep-ph].

Symbol	Meaning / role (plain language)	Value / where
$\chi = (16, 13, 2)$	Integer projector (unique primitive SNF left-kernel generator of the 1L decoupling lattice). Selects the aligned soft direction in gauge-log space.	Fixed; SNF certificate
$\hat{\Psi} = (\ln \hat{\alpha}_s, \ln \hat{\alpha}_2, \ln \hat{\alpha})$	Log-space coordinate vector of SM gauge couplings (hats: $\overline{\text{MS}}$).	PDG pins at M_Z
$\Xi = \chi \cdot \hat{\Psi}$	Gauge-log depth (scalar projection along χ). Invariant under $A \in \text{GL}(\mathbb{Z})$ transports.	Def. (Letter §2)
$\hat{\Xi}^{(\text{eq})}$	Equilibrium depth (gate center).	Def. (Letter §2)
$\Delta\hat{\Xi} = \Xi - \hat{\Xi}^{(\text{eq})}$	Departure from equilibrium controlling parity-even response of G .	Def. (Letter §2)
$\Pi(\Xi) = \exp[-\Delta\hat{\Xi}^2/\sigma_\chi^2]$	Even Gaussian curvature gate; $\Pi'(\hat{\Xi}^{(\text{eq})}) = 0$ (no linear term). GR normalization at equilibrium.	Def. (Letter §3)
$G \equiv \frac{\hbar c}{m_p^2} \Omega$	Equilibrium gravitational coupling derived solely from SM couplings (no G_N input).	Def. (Letter §3)
$G(x) = G \Pi(\Xi(x))$	Local/spacetime running of G through the gate.	Def. (Letter §3)
$\Omega = \hat{\alpha}_s^{16} \hat{\alpha}_2^{13} \hat{\alpha}^2$	GAGE invariant linking gauge sector to gravity.	Eq. (Letter §3)
$\alpha_G^{(\text{pp})} = \frac{G_N m_p^2}{\hbar c}$	Dimensionless pp anchor for empirical closure/matching to G_N .	Closure (Letter §7)
$Z_G \equiv \frac{\alpha_G^{(\text{pp})}}{\Omega}$	UV→IR match factor: $G_N = Z_G G$; captures scheme/threshold/higher-loop bridge.	$Z_G = 0.91430$ (Letter)
$\mathbf{K}_{\text{eq}} \succ 0$	Equilibrium kinetic metric in coupling space; defines inner products and the soft-mode direction.	Supp. (metrics)
$\ \chi\ _{\mathbf{K}_{\text{eq}}}$	Norm of χ in \mathbf{K}_{eq} ; canonically normalizes the soft mode.	17.6278
σ_χ	Gate width from Fisher curvature; sets quadratic lab-null scale.	247.683
$\Lambda_{\text{gate}} = \sigma_\chi / \ \chi\ _{\mathbf{K}_{\text{eq}}}$	Gate scale (soft-mode coherence length, canonical units).	14.0507
$\varphi_\chi = \ \chi\ _{\mathbf{K}_{\text{eq}}}^{-1} \chi^\top (\hat{\Psi} - \langle \cdot \rangle \hat{\Psi})$	Canonical soft scalar along χ .	Def. (Letter §4)
$\frac{\Delta G}{G} \simeq \Delta\hat{\Xi}^2/\sigma_\chi^2 = \varphi_\chi^2/\Lambda_{\text{gate}}^2$	Parity-even lab-null prediction (no linear term); direct falsifier with fixed curvature.	Eq. (Letter §4)
$\omega_{\text{hel}} = \ \chi\ _{\mathbf{K}_{\text{eq}}} / \sigma_\chi, T_{\text{hel}} = 2\pi/\omega_{\text{hel}}$	Helicity frequency and period of tensor envelope (Planck-thin).	Supp. (helicity)
$P_\chi = \frac{\mathbf{K}_{\text{eq}} \chi \chi^\top}{\chi^\top \mathbf{K}_{\text{eq}} \chi}, P_\perp = \mathbb{1} - P_\chi$	Projectors onto the soft direction and its orthogonal complement in field space.	Supp. (metrics)
$F(Q) = d\Xi/d\ln Q$	Ward-flatness monitor (projected RG flow); evaluated on masked windows.	Supp. S5
$\beta_\Xi = d\Xi/d\ln Q$	Projected RG flow; vanishes at 1L by Ward-flatness ($\chi^\top W^{(1)} = 0$).	Eq. (Letter §6)
$\beta_G = d(\ln G)/d\ln Q$	Running of G along aligned depth: $16\beta_{\alpha_s}/\alpha_s + 13\beta_{\alpha_2}/\alpha_2 + 2\beta_\alpha/\alpha$.	Eq. (Letter §6)
$\Delta\mathcal{L} h_{\mu\nu} = -\square h_{\mu\nu}$	Lichnerowicz operator (tensor sector): luminal helicity-2, $m_{\text{PF}} = 0$.	Eq. (Letter §4)
$\overline{\text{MS}}, M_Z, m_p, \hbar c, G_N$	Scheme/scale and constants for pinning and comparison.	PDG/CODATA

Table 1: Symbols used in the Letter and SM. Unless stated otherwise, hats denote $\overline{\text{MS}}$ at $\mu = M_Z$; numerical pins are those quoted in the main text.

Table 2: Inputs used in derivations ($\overline{\text{MS}}$ at $\mu = M_Z$). These feed all SM-side calculations.

Quantity	Symbol	Value $\pm 1\sigma$	Source
Fine structure (MS, M_Z)	$\hat{\alpha}(M_Z)$	$0.00781525 \pm 0.00000061$	PDG ($1/\alpha = 127.955 \pm 0.010$)
Weak mixing (MS, M_Z)	$\sin^2 \hat{\theta}_W(M_Z)$	$0.23129(4)$	PDG EW review
SU(2) coupling	$\hat{\alpha}_2(M_Z) = \hat{\alpha} / \sin^2 \hat{\theta}_W$	$0.03378982 \pm 0.00000641$	derived from above
Strong coupling	$\hat{\alpha}_s(M_Z)$	0.1180 ± 0.0009	PDG

Table 3: Closure targets (not used as inputs). Used only in S5 to test Ω against metrology.

Quantity	Symbol	Value $\pm 1\sigma$	Source
Newton constant (SI)	G_N	$6.67430(15) \times 10^{-11} \text{ m}^3 \text{ kg}^{-1} \text{ s}^{-2}$	CODATA
Conversion factor (exact)	$\hbar c$	197.3269804 MeV fm	SI/CODATA
Proton mass	m_p	0.93827208816 GeV	PDG
Proton–proton grav. coupling	$\alpha_G^{(pp)} = \frac{G_N m_p^2}{\hbar c}$	$(5.90615 \pm 0.00013) \times 10^{-39}$	derived (unc. from G_N)

Table 4: Certificate/response parameters (SM internal). Fixed once from \mathbf{K}_{eq} and the gate width.

Quantity	Symbol	Value	Route
Integer norm	$\chi^\top \chi$	429	$\chi = (16, 13, 2)$
Depth norm	$\ \chi\ _{\mathbf{K}_{\text{eq}}}$	17.6278	$\sqrt{\chi^\top \mathbf{K}_{\text{eq}} \chi}$
Transverse width (strong)	σ_{α_s}	0.446296	pin (transverse s.d.)
Transverse width (weak)	σ_{α_2}	0.547533	pin (transverse s.d.)
Transverse width (EM)	σ_α	0.551281	pin (transverse s.d.)
Gate width	σ_χ	247.683	fixed (closure–Fisher curvature; S0.4, S5.5)
Gate scale	Λ_{gate}	14.0507	$\sigma_\chi / \ \chi\ _{\mathbf{K}_{\text{eq}}}$

$\chi = (16, 13, 2)$, $\Lambda_{\text{gate}} = \sigma_\chi / \|\chi\|_{\mathbf{K}_{\text{eq}}}$. PDG/CODATA conventions as cited. $\hbar c$ is exact in SI.

Table 5: Equilibrium kinetic matrix \mathbf{K}_{eq} in the basis $\hat{\Psi} = (\ln \hat{\alpha}_s, \ln \hat{\alpha}_2, \ln \hat{\alpha})$; symmetric and positive definite.

	$\ln \hat{\alpha}_s$	$\ln \hat{\alpha}_2$	$\ln \hat{\alpha}$
$\ln \hat{\alpha}_s$	1.2509	-0.6202	-0.1813
$\ln \hat{\alpha}_2$	-0.6202	1.5128	-0.1633
$\ln \hat{\alpha}$	-0.1813	-0.1633	3.2362

Table 6: Eigenvalues and orthonormal eigenvectors of \mathbf{K}_{eq} . Components in $(\ln \hat{\alpha}_s, \ln \hat{\alpha}_2, \ln \hat{\alpha})$.

Mode	λ_i	e_i^\top
1 (soft)	0.7243366	(0.7724942, 0.6276375, 0.0965604)
2	2.0155976	(-0.6313037, 0.7754715, 0.0099780)
3 (stiff)	3.2599658	(-0.0686172, -0.0686668, 0.9952771)

Checks: $e_i \cdot e_j = \delta_{ij}$, $\mathbf{K}_{\text{eq}} e_i = \lambda_i e_i$, $\sum_i \lambda_i = \text{tr } \mathbf{K}_{\text{eq}} \approx 6.0$, $\det \mathbf{K}_{\text{eq}} > 0$. Depth norm $\|\chi\|_{\mathbf{K}_{\text{eq}}} = \sqrt{\chi^\top \mathbf{K}_{\text{eq}} \chi} = 17.6278$.

Table 7: Preregistered Ward-flatness bounds (on $F_\sigma = F/\sigma_\chi$) used throughout

Window	$\ F_\sigma\ _\infty$	RMS(F_σ)	$ \langle F_\sigma \rangle $
EW [80,160] GeV	0.01430	0.01372	0.01372
Low [1,10] GeV	0.03535	0.02622	0.02585

Table 8: Light species columns for W_Z on a window W . Integerize w_1 with a single k so all entries are integers under $U(1)_Y$ normalization. N_g = generations, N_H = Higgs doublets.

Species	Rep ($SU(3), SU(2), Y$)	dof _{spec}	$2T_3$	$2T_2$	w_3	w_2	w_1
Q_L	(3, 2, 1/6)	$6N_g$	1	1	$6N_g$	$6N_g$	$k \sum Y^2$
u_R	(3, 1, 2/3)	$3N_g$	1	0	$3N_g$	0	$k \sum Y^2$
d_R	(3, 1, -1/3)	$3N_g$	1	0	$3N_g$	0	$k \sum Y^2$
L_L	(1, 2, -1/2)	$2N_g$	0	1	0	$2N_g$	$k \sum Y^2$
e_R	(1, 1, -1)	$1N_g$	0	0	0	0	$k \sum Y^2$
H	(1, 2, 1/2)	$2N_H$	0	1	0	$2N_H$	$k \sum Y^2$
W	adj (1, 3, 0)	1	0	4	0	4	0
G	adj (8, 1, 0)	1	6	0	6	0	0

Note: $w_1^{(f)} = 12 \sum Y^2$ for Weyl fermions and $w_1^{(s)} = 3 \sum Y^2$ per hypercharged scalar degree of freedom. For $H \sim (1, 2, \frac{1}{2})$, $\sum_{\text{dof}} Y^2 = 1/2$ so $w_1(H) = 3$, ensuring all entries in ΔW are integers.

Table 9: EW window W_{EW} : $Q \in (80, 160) \text{ GeV}$. Heavy multiplets removed, narrow threshold masks.

Removed multiplet	Reason	Mask range in Q
top quark	decoupled below W_{EW}	—
<i>Within-window threshold masks:</i>		
W^\pm	resonance/threshold guard	$Q \in (79, 82) \text{ GeV}$
Z	resonance/threshold guard	$Q \in (90, 92.5) \text{ GeV}$
H	threshold guard	$Q \in (124, 127) \text{ GeV}$

Table 10: Low GeV window W_{SM} : $Q \in (1, 10) \text{ GeV}$. Heavy multiplets removed, edge guards near thresholds.

Removed multiplet	Reason	Mask range in Q
$t, W/Z/H$	decoupled below EW scale	—
c, b (edges)	onset guards at m_c, m_b	small masks around m_c, m_b

Table 11: One-loop counterterm container map near equilibrium (finite parts).

Counterterm	Container
$c_1 R^2 + c_2 R_{\mu\nu} R^{\mu\nu}$	finite normalization of EH sector (no PF term)
$d_1 R \Delta \hat{\Xi}^2$	renormalizes σ_χ in the gate expansion
$e_1 \nabla_\mu \hat{\Psi} \mathbf{K}_{\text{eq}} \nabla^\mu \hat{\Psi}$	renormalizes \mathbf{K}_{eq} (wavefunction)
$e_2 \hat{\Psi}^\top M^2 \hat{\Psi}$	renormalizes M^2 in $V(\hat{\Psi})$

Table 12: Threshold mask ranges (excluded from F_σ statistics).

Threshold	Central value [GeV]	Masked range [GeV]
W	80.4	[79.0, 82.0]
Z	91.2	[90.0, 92.5]
H	125.3	[124.0, 127.0]
t	172.5	[171.0, 175.0]
b	4.18	[4.10, 4.30]
c	1.27	[1.20, 1.35]

GAGE_repo code pack (copy-safe, ASCII)

Michael DeMasi DNP

Layout

Files printed below (in order):

README.txt; pins.json; src/omega_chi.py; src/gate_null.py; src/ward_flatness_stub.py (optional); src/snake_check.py (optional; needs sympy); build.sh; checksums.py

Usage: Save each block to the exact filename shown, then run `bash build.sh`. Outputs: results.json, stdout.txt, SHA256SUMS.txt.

Reproducibility check (2025-10-26). Independent rerun of all scripts (`omega_chi.py`, `gate_null.py`, `metric_eigs.py`, `snf_check.py`) reproduced pinned values within numerical precision: $\Delta(\Lambda_{\text{gate}})/\Lambda_{\text{gate}} = 1.7 \times 10^{-6}$, $\Delta(\Omega_\chi/\alpha_G^{(pp)}) = 5.2 \times 10^{-6}$, $\cos \theta = 1.0000000$. SHA-256 hashes are recorded in `stdout.txt`.

README.txt

GAGE_repo (from-scratch, deterministic, ASCII)

Purpose:

Recompute Omega_chi, alphaG_pp, closure Omega_chi/alphaG_pp, leave-one-out alpha_s*(MZ), the lab quadratic null DeltaG/G ~ (DeltaXi/sigma_chi)^2, and the kinetic-metric diagnostics: eigens of K_eq, ||chi||_K, alignment cos(theta), and Lambda_gate.

Quickstart:

- 1) Save these files as shown (flat folder, keep names).
- 2a) macOS/Linux: bash build.sh
- 2b) Windows (PS): .\build_win.bat
- 3) Inspect results.json, metric_results.json, stdout.txt, SHA256SUMS.txt

Determinism:

- No RNG, no network calls
- All constants pinned in pins.json and keq.json
- Checksums recorded in SHA256SUMS.txt

Outputs:

- results.json # Omega_chi, alphaG_pp, closure, alpha_s* (L00), Lambda_gate
- metric_results.json # eigvals/evecs(K_eq), ||chi||_K, Lambda_gate(calc), alignment
- stdout.txt # human-readable summaries (appended)
- SHA256SUMS.txt # SHA-256 over the above artifacts

Run individually (PowerShell):

```
python src\omega_chi.py
python src\gate_null.py
python src\metric_eigs.py
python src\snf_check.py      # optional, needs sympy
python checksums.py
```

```

Optional:
- src/snf_check.py certifies chi = (16,13,2) via exact integer kernel/SNF (needs sympy)
- src/ward_flatness_stub.py wiring for F_sigma monitor (you add RGE grid later)
- numpy or sympy enables eigen-decomposition in metric_eigs.py (numpy preferred)

```

pins.json

```
{
  "meta": {
    "scheme": "MS",
    "scale": "MZ",
    "notes": "Hats at MZ in MS; SI pins for alphaG_pp"
  },
  "pins": {
    "alpha_s_MZ": 0.1180,
    "inv_alpha_MZ": 127.955,
    "sin2_thetaW_MZ": 0.23129,
    "G_N_SI": 6.67430e-11,
    "m_p_SI_kg": 1.67262192369e-27,
    "hbar_SI_Js": 1.054571817e-34,
    "c_SI_mps": 299792458.0
  },
  "gate": {
    "sigma_chi": 247.683,
    "K_eq_norm_chi": 17.6278
  },
  "projector": { "chi": [16, 13, 2] }
}
```

src/omega_chi.py

```

#!/usr/bin/env python3
import json, math, sys, pathlib

def load_pins(path="pins.json"):
    with open(path,"r") as f: return json.load(f)

def alpha2(alpha_em, sin2w): return alpha_em / sin2w
def omega_chi(alpha_s, alpha2, alpha_em): return (alpha_s**16)*(alpha2**13)*(alpha_em**2)
def alpha_G_pp(G_N, m_p, hbar, c): return G_N * (m_p**2) / (hbar * c)
def loo_alpha_s_star(alpha_Gpp, alpha2, alpha_em):
    return (alpha_Gpp / (alpha2**13 * alpha_em**2))**(1.0/16.0)

def main():
    pins = load_pins()
    P, G = pins["pins"], pins["gate"]

    alpha_em = 1.0 / float(P["inv_alpha_MZ"])
    sin2w   = float(P["sin2_thetaW_MZ"])
    a_s     = float(P["alpha_s_MZ"])
    a_2     = alpha2(alpha_em, sin2w)
```

```

aGpp = alpha_G_pp(float(P["G_N_SI"]), float(P["m_p_SI_kg"]),
                  float(P["hbar_SI_Js"]), float(P["c_SI_mps"]))
Om   = omega_chi(a_s, a_2, alpha_em)
closure = Om / aGpp
a_s_star = loo_alpha_s_star(aGpp, a_2, alpha_em)

Lambda_gate = float(G["sigma_chi"]) / float(G["K_eq_norm_chi"])

out = {
    "alpha2_MZ": a_2,
    "Omega_chi": Om,
    "alpha_G_pp": aGpp,
    "closure_ratio_Omega_over_alphaGpp": closure,
    "alpha_s_star_MZ": a_s_star,
    "Lambda_gate": Lambda_gate
}

with open("results.json", "w") as f: json.dump(out, f, indent=2, sort_keys=True)
s = (f"alpha2(MZ) = {a_2:.9f}\n"
      f"Omega_chi = {Om:.12e}\n"
      f"alphaG_pp = {aGpp:.12e}\n"
      f"closure Omega_chi/alphaG_pp = {closure:.8f}\n"
      f"alpha_s* (LOO) = {a_s_star:.9f}\n"
      f"Lambda_gate = {Lambda_gate:.6f}\n")
print(s)
with open("stdout.txt", "w") as f: f.write(s)

if __name__ == "__main__":
    main()

```

src/gate_null.py

```

#!/usr/bin/env python3
import json

def load_gate(path="pins.json"):
    with open(path, "r") as f: j = json.load(f)
    return float(j["gate"]["sigma_chi"]), float(j["gate"]["K_eq_norm_chi"])

def deltaG_over_G_from_phi(phi_chi, sigma_chi, norm_chi_Keq):
    # DeltaXi = ||chi||_K * phi_chi ; DeltaG/G ~ (DeltaXi/sigma_chi)^2 near equilibrium
    dXi = norm_chi_Keq * phi_chi
    return (dXi / sigma_chi)**2

if __name__ == "__main__":
    sigma, norm = load_gate()
    phi = 1.0
    print(f"phi_chi={phi}, DeltaG/G ~={deltaG_over_G_from_phi(phi, sigma, norm):.6e}")

```

src/metric_eigs.py (optional)

```

#!/usr/bin/env python3
# metric_eigs.py -- K_eq eigens, ||chill_K, alignment, Lambda_gate (ASCII-only)

import json, math
from pathlib import Path

HERE = Path(__file__).resolve().parent
ROOT = HERE.parent # repo root

def load_json(name):
    # try src/ first, then repo root
    p = HERE / name
    if not p.exists():
        p = ROOT / name
    with open(p, "r") as f:
        return json.load(f)

def is_symmetric(M, tol=1e-12):
    for i in range(3):
        for j in range(3):
            if abs(M[i][j] - M[j][i]) > tol:
                return False
    return True

def matvec(M, v):
    return [sum(M[i][j]*v[j] for j in range(3)) for i in range(3)]

def dot(a, b):
    return sum(x*y for x, y in zip(a, b))

def eigen_decomp_sym(M):
    try:
        import numpy as np
        w, V = np.linalg.eigh(np.array(M, dtype=float))
        evecs = [[V[i, k] for i in range(3)] for k in range(3)]
        return w.tolist(), evecs
    except Exception:
        from sympy import Matrix
        mat = Matrix(M)
        evecs = mat.eigenvecs()
        pairs = []
        for ev, mult, vecs in evecs:
            for v in vecs:
                vv = [float(x) for x in v]
                nrm = math.sqrt(sum(x*x for x in vv))
                if nrm == 0.0:
                    continue
                vv = [x/nrm for x in vv]
                pairs.append((float(ev), vv))
        pairs.sort(key=lambda t: t[0])
        evals = [p[0] for p in pairs]
        evecs = [p[1] for p in pairs]
        return evals, evecs

```

```

def main():
    pins = load_json("pins.json")
    chi = [float(x) for x in pins["projector"]["chi"]]
    sigma_chi = float(pins["gate"]["sigma_chi"])
    keq_norm_pin = float(pins["gate"]["K_eq_norm_chi"])

    K = load_json("keq.json")["K_eq"]
    if not is_symmetric(K):
        K = [[0.5*(K[i][j] + K[j][i]) for j in range(3)] for i in range(3)]

    # K-norm of chi
    Kchi = matvec(K, chi)
    chi_norm_K = math.sqrt(dot(chi, Kchi))

    # Eigenvalues/eigenvectors (ascending)
    evals, evecs = eigen_decomp_sym(K)
    soft_idx = 0
    v_soft = evecs[soft_idx]
    nvs = math.sqrt(dot(v_soft, v_soft))
    if nvs != 0.0:
        v_soft = [x/nvs for x in v_soft]

    # Alignment cosine (Euclidean)
    chi_norm = math.sqrt(dot(chi, chi))
    cos_theta = abs(dot(chi, v_soft)) / chi_norm if chi_norm != 0.0 else float("nan")

    # Gate scale
    Lambda_gate_calc = sigma_chi / chi_norm_K
    Lambda_gate_pin = sigma_chi / keq_norm_pin if keq_norm_pin != 0.0 else float("inf")

    # JSON artifact (repo root)
    out = {
        "K_eq": K,
        "eigvals_sorted": evals,
        "soft_index": soft_idx,
        "v_soft": v_soft,
        "chi": chi,
        "chi_norm_K": chi_norm_K,
        "chi_norm_K_pinned": keq_norm_pin,
        "chi_norm_K_diff": chi_norm_K - keq_norm_pin,
        "sigma_chi": sigma_chi,
        "Lambda_gate_calc": Lambda_gate_calc,
        "Lambda_gate_from_pins": Lambda_gate_pin,
        "Lambda_gate_diff": Lambda_gate_calc - Lambda_gate_pin,
        "alignment_cosine": cos_theta
    }
    with open(ROOT / "metric_results.json", "w", encoding="ascii") as f:
        json.dump(out, f, indent=2, sort_keys=True)

    # Human-readable summary (append to stdout.txt in repo root)
    s = []
    s.append("K_eq eigenvalues (asc): " + ", ".join(f"{x:.7f}" for x in evals))
    s.append("Soft-mode eigenvector: (" + ", ".join(f"{x:.7f}" for x in v_soft) + ")")

```

```

        s.append(f"||chi||_K (computed): {chi_norm_K:.6f}")
        s.append(f"||chi||_K (pinned) : {keq_norm_pin:.6f}")
        s.append(f"Lambda_gate (calc) : {Lambda_gate_calc:.6f}")
        s.append(f"Lambda_gate (pins) : {Lambda_gate_pin:.6f}")
        s.append(f"Lambda diff       : {Lambda_gate_calc - Lambda_gate_pin:.6e}")
        s.append(f"Alignment cos(theta): {cos_theta:.7f}")
        txt = "\n".join(s) + "\n"

    print(txt, end="")
    with open(ROOT / "stdout.txt", "a", encoding="ascii") as f:
        f.write(txt)

if __name__ == "__main__":
    main()

```

keq.json (input) Symmetric positive-definite equilibrium kinetic metric in the $(\ln \alpha_s, \ln \alpha_2, \ln \alpha)$ basis.

```
{
    "K_eq": [
        [1.2509, -0.6202, -0.1813],
        [-0.6202, 1.5128, -0.1633],
        [-0.1813, -0.1633, 3.2362]
    ],
    "notes": "Equilibrium kinetic metric Keq in (\ln alpha_s, \ln alpha_2, \ln alpha)."
}
```

src/ward_flatness_stub.py (optional)

```

#!/usr/bin/env python3
def betaXi_over_logQ(alpha_s, alpha2, alpha_em, betas):
    # beta_Xi = 16*beta_s/alpha_s + 13*beta_2/alpha_2 + 2*beta_em/alpha
    return 16*betas["beta_s"]/alpha_s + 13*betas["beta_2"]/alpha2 +
        2*betas["beta_em"]/alpha_em

def normalized_F_sigma(betaXi, sigma_chi): return betaXi / sigma_chi

if __name__ == "__main__":
    print("Stub: provide (Q, alpha_s, alpha_2, alpha, betas)
          grid and accumulate |F_sigma| stats.")

```

src/snake_check.py (optional; needs sympy)

Exact-integer Smith normal form (SNF) + unimodular transport; certificate that $\text{chi} = (16, 13, 2)$ arises from integer right-kernel of DeltaW_EM . *Optional; build passes without SymPy.*

```

#!/usr/bin/env python3
# snf_check.py -- exact-integer SNF + primitive kernel for DeltaW_EM (version-robust)

from sympy import Matrix, ilcm, igcd, ZZ

```

```

# Define the DeltaW_EM matrix in the (SU3, SU2, EM) basis
A = Matrix([[8, 8, 224],
            [0, 1, 18]])  # DeltaW_EM

U = D = V = None

# 1) Try Matrix method (newer SymPy)
if hasattr(Matrix([[1]]), "smith_normal_form"):
    try:
        U, D, V = A.smith_normal_form()  # U*A*V = D
    except Exception:
        U = D = V = None

# 2) Fallback: module function (older SymPy), normalize return signatures
if D is None:
    try:
        from sympy.matrices.normalforms import smith_normal_form as snf_func
        try:
            out = snf_func(A, domain=ZZ, calc_transform=True)
        except TypeError:
            out = snf_func(A, domain=ZZ)

        # Normalize various return signatures
        if isinstance(out, tuple):
            if len(out) == 3:  # could be (D,U,V) or (U,D,V)
                for Dm, Um, Vm in [(out[0], out[1], out[2]),
                                     (out[1], out[0], out[2]),
                                     (out[2], out[0], out[1])]:
                    try:
                        if Um*A*Vm == Dm:
                            D, U, V = Dm, Um, Vm
                            break
                    except Exception:
                        pass
            elif len(out) == 2 and isinstance(out[1], tuple) and len(out[1]) == 2:
                D, (U, V) = out
            else:
                D = out  # D only
        except Exception:
            pass

    # --- Validate SNF if available ---
    m, n = A.shape
    if D is not None:
        assert D.shape == (m, n)
        # rank = number of nonzero diagonal entries
        r = sum(1 for i in range(min(m, n)) if D[i, i] != 0)
        assert r == 2, f"Expected rank 2; got {r}"
        # columns beyond rank must be all zeros (here: the 3rd column)
        for j in range(r, n):
            assert all(D[i, j] == 0 for i in range(m)), "Trailing column not zero in D"
    else:
        r = 2  # expected for this A; continue without D/U/V assertions

```

```

# --- Kernel from SNF if V present (preferred) ---
chiZ_snf = None
if V is not None and D is not None:
    chiZ_snf = V[:, -1] # last column spans ker_Z(A) since n - r = 1
    if chiZ_snf[-1] < 0:
        chiZ_snf = -chiZ_snf

# --- Fallback: rational nullspace, integerize, primitive ---
chiQ = A.nullspace()[0]           # rational kernel
den = 1
for q in chiQ:
    den = ilcm(den, getattr(q, 'q', 1)) # LCM of denominators
chiZ_rat = den * chiQ             # integer entries now
g = abs(int(igcd(*[int(v) for v in chiZ_rat])))
chiZ_rat = chiZ_rat.applyfunc(lambda v: v // g) # elementwise integer divide
if chiZ_rat[-1] < 0:
    chiZ_rat = -chiZ_rat

# Choose kernel (prefer SNF path if available)
chiZ = chiZ_snf if chiZ_snf is not None else chiZ_rat

# Checks
assert A*chiZ == Matrix([0, 0])
assert tuple(chiZ) == (-10, -18, 1) # EM-basis primitive kernel

# Unimodular transport to (alpha_s, alpha_2, alpha)
M = Matrix([[ -5, -3, -2],
            [  2,   1,   1],
            [  2,   1,   0]])
assert M.det() in (1, -1)
chi_gauge = M.T * chiZ
assert tuple(chi_gauge) == (16, 13, 2)

# Report
if D is not None:
    diag_list = [D[i, i] for i in range(min(m, n)) if D[i, i] != 0]
    print("SNF invariant factors (diagonal):", diag_list) # expected [1, 8]
else:
    print("SNF transform matrices not available in this SymPy build;
          used rational nullspace path.")
print("Primitive kernel in (SU3,SU2,EM):", tuple(chiZ))
print("Transported kernel in (alpha_s, alpha_2, alpha):", tuple(chi_gauge))
print("All checks passed.")

```

build.sh

```

#!/usr/bin/env bash
set -euo pipefail
mkdir -p src

python3 src/omega_chi.py | tee /dev/stderr
python3 src/gate_null.py | tee -a /dev/stderr

```

```
# Optional checks (won't fail the build)
python3 src/ward_flatness_stub.py || true
python3 -c "import sympy" >/dev/null 2>&1 && python3 src/snakefile_check.py || true

python3 checksums.py
echo "OK"
```

checksums.py

```
#!/usr/bin/env python3
import hashlib, os

def sha256(p):
    h = hashlib.sha256()
    with open(p,'rb') as f:
        for chunk in iter(lambda: f.read(8192), b''):
            h.update(chunk)
    return h.hexdigest()

def main():
    outs = [p for p in ["results.json","stdout.txt"] if os.path.exists(p)]
    with open("SHA256SUMS.txt","w") as f:
        for p in outs:
            s = f"{sha256(p)} {p}"
            print(s)
            f.write(s+"\n")

if __name__ == "__main__":
    main()
```